



UNIVERSITY OF LEEDS

This is a repository copy of *Selective Enhancement of Insulin Sensitivity in the Endothelium In Vivo Reveals a Novel Proatherosclerotic Signaling Loop*.

White Rose Research Online URL for this paper:
<http://eprints.whiterose.ac.uk/109437/>

Version: Accepted Version

Article:

Viswambharan, VH orcid.org/0000-0002-7616-5026, Yuldasheva, NY orcid.org/0000-0001-6213-6358, Sengupta, A et al. (18 more authors) (2017) Selective Enhancement of Insulin Sensitivity in the Endothelium In Vivo Reveals a Novel Proatherosclerotic Signaling Loop. *Circulation Research*, 120 (5). pp. 784-798. ISSN 0009-7330

<https://doi.org/10.1161/CIRCRESAHA.116.309678>

© 2016 American Heart Association, Inc. This is an author produced version of a paper published in *Circulation Research*. Uploaded in accordance with the publisher's self-archiving policy.

Reuse

Items deposited in White Rose Research Online are protected by copyright, with all rights reserved unless indicated otherwise. They may be downloaded and/or printed for private study, or other acts as permitted by national copyright laws. The publisher or other rights holders may allow further reproduction and re-use of the full text version. This is indicated by the licence information on the White Rose Research Online record for the item.

Takedown

If you consider content in White Rose Research Online to be in breach of UK law, please notify us by emailing eprints@whiterose.ac.uk including the URL of the record and the reason for the withdrawal request.



eprints@whiterose.ac.uk
<https://eprints.whiterose.ac.uk/>

Selective Enhancement of Insulin Sensitivity in the Endothelium In Vivo Reveals a Novel Proatherosclerotic Signalling Loop.

First Author's Surname: Viswambharan

Short Title: Insulin sensitivity and NO availability

Hema Viswambharan PhD*, Nadira Yuldasheva PhD, Anshuman Sengupta MBChB PhD, Helen Imrie PhD, ¹Matthew Gage PhD, Natalie Haywood PhD, Andrew MN Walker MBChB, Anna Skromna MSc, Natallia Makova MSc, Stacey Galloway BSc, Pooja Shah BSc, Piruthivi Sukumar PhD, Karen E Porter PhD, Peter J Grant MD FMedSci, ²Ajay M Shah MD FMedSci, ¹Celio XC Santos PhD, Jing Li PhD, David J Beech PhD FMedSci, Stephen B Wheatcroft MBBS FRCP, Richard M Cubbon MBChB PhD, Mark T Kearney DM FRCP.

Leeds Institute of Cardiovascular and Metabolic Medicine, University of Leeds. ¹Metabolism & Experimental Therapeutics, Division of Medicine, University College London. ²British Heart Foundation Centre of Research Excellence, King's College London.

Address for Correspondence and person to whom reprint requests should be addressed:

Dr. Hema Viswambharan*
Leeds Institute of Cardiovascular and Metabolic Medicine,
University of Leeds,
Clarendon Way,
Leeds, LS2 9JT,
United Kingdom.
Email: h.viswambharan@leeds.ac.uk
Tel: +441133437764
Fax: +441133437738

Additional Footnotes:

Present address of Matthew Gage: Metabolism and Experimental Therapeutics, Faculty of Medical Sciences, University College London, London, United Kingdom.

Word Count: 9776 words

Subject Code List: Vascular biology [95] Endothelium/vascular type/nitric oxide, Diabetes [190] Type 2 Diabetes

Abstract

Rationale: In the endothelium, insulin stimulates endothelial nitric oxide synthase (eNOS) to generate the anti-atherosclerotic signalling radical NO. Insulin resistant type 2 diabetes is associated with reduced NO availability and accelerated atherosclerosis. The effect of enhancing endothelial insulin sensitivity on NO availability is unclear.

Objective: To answer this question we generated a mouse with endothelial cell (EC)-specific over-expression of the human insulin receptor (hIRECO) using the Tie2 promoter-enhancer.

Methods and Results: hIRECO demonstrated significant endothelial dysfunction measured by blunted endothelium-dependent vasorelaxation to acetylcholine which was normalized by a specific Nox2 NADPH oxidase inhibitor. Insulin-stimulated phosphorylation of Akt was increased in hIRECO EC as was Nox2 NADPH oxidase-dependent generation of superoxide, whereas insulin and shear stress-stimulated eNOS activation were blunted. Phosphorylation at the inhibitory residue Y657 of eNOS and expression of PYK2 which phosphorylates this residue were significantly higher in hIRECO EC. Inhibition of PYK2 improved insulin and shear-induced eNOS activation in hIRECO EC.

Conclusions: Enhancing insulin sensitivity specifically in EC leads to a paradoxical decline in endothelial function, mediated by increased tyrosine phosphorylation of eNOS and excess Nox2 derived superoxide. Increased EC insulin sensitivity leads to a pro-atherosclerotic imbalance between NO and superoxide. Inhibition of PYK2 restores insulin- and shear-induced NO production. This study demonstrates for the first time that increased endothelial insulin sensitivity leads to a pro-atherosclerotic imbalance between NO and superoxide.

Key Words: Insulin; Insulin Resistance; Endothelial Dysfunction; PYK2; Reactive oxygen Species; Superoxide

Non-standard Abbreviations and Acronyms: NO-nitric oxide, hIR-human Insulin Receptor; hIRECO- endothelial cell (EC)-specific over-expression of the human insulin receptor; EC-endothelial cells; PEC-pulmonary endothelial cells; PYK2-proline-rich tyrosine kinase 2; Akt-protein kinase B; ACh-acetylcholine; PE-phenylephrine; SNP-sodium nitroprusside; eNOS-endothelial nitric oxide synthase.

Introduction

Recent changes in human lifestyle have led to a global epidemic of type 2 diabetes mellitus.¹ Type 2 diabetes mellitus is characterized by hyperinsulinaemic insulin resistance,² a situation whereby insulin is unable to activate its intricate intracellular signalling network in an appropriate temporospatial fashion.³ Insulin resistance results in a loss of protection against a range of chronic disorders of human health, principal amongst which is atherosclerosis.⁴ A key step in the initiation and progression of atherosclerosis is the deleterious change in endothelial cell phenotype, characterised by an imbalance between the anti-atherosclerotic signalling radical nitric oxide (NO) and generation of the potentially cytotoxic free radical superoxide, a scenario described as endothelial dysfunction.⁵

There is a compelling body of evidence from studies in endothelial cells *in vitro* demonstrating that insulin, by acting on its tyrosine kinase receptor, stimulates production of NO,⁶ inhibits superoxide generation, blunts inflammatory cell recruitment and inhibits thrombosis.⁷ *In vivo* models of insulin resistance at a whole body level,⁸ and at the level of the endothelium,^{9,10} have confirmed the hypothesis that insulin resistance *per se* leads to a reduced level of NO, excessive generation of superoxide and accelerated atherosclerosis.

While we appreciate the effects of whole body and cell-specific insulin resistance on the development of atherosclerosis, the local and systemic consequences of prolonged insulin signalling in the endothelium are poorly understood. Therefore, in order to improve our mechanistic understanding of the impact of selectively enhancing insulin action in the endothelium on the development of atherosclerosis, from its earliest biochemical manifestation of reduced NO availability, to lipid deposition and structural changes in the arterial wall, we have generated a transgenic mouse model over-expressing the human insulin receptor (IR) specifically in the endothelium. For the first time, we demonstrate that endothelial cell over-expression of IR enhances insulin-stimulated activation of the kinase Akt, which increases activity of the superoxide generating enzyme Nox2 NADPH oxidase. Additionally, over-expression of IR also increases expression of proline rich tyrosine kinase (PYK2), a negative regulator of endothelial NO synthase (eNOS).¹¹ In the presence of enhanced insulin signalling, crosstalk between Nox2 and PYK2 increases their expression further, thus amplifying the deleterious effect of prolonged enhancement of endothelial cell insulin signalling on the critical balance between NO and superoxide levels. Taking these findings further, we crossed transgenic mice with endothelium-specific expression of the IR onto an atherosclerosis-prone apolipoprotein E deficient background. Interestingly, these mice developed accelerated atherosclerosis. Our findings demonstrate that enhanced and prolonged insulin signalling specifically in the endothelium, establishes a deleterious feed-forward circuit involving: IR, Akt, Nox2, PYK2 and eNOS, leading to endothelial dysfunction and accelerated atherosclerosis.

Methods

Mice over-expressing the human insulin receptor specific to the endothelium. To examine the local and systemic consequences of prolonged enhancement of insulin sensitivity in the endothelium we generated a transgenic mouse with endothelium specific over expression of the type A isoform of the human IR (Supplemental Figure IA). Mice were bred onto a C57BL/6J background to at least 10 generations in a conventional animal facility with a 12-h light/dark cycle. Male mice aged 3-4 months were used in all experiments, which were conducted in accordance with accepted ethical standards of humane animal care (UK Animals Scientific Procedure Act 1986) under United Kingdom Home Office Project License No. 40/2988.

To overcome the limitations seen in standard transgenics we used the Hypoxanthine Phosphoribosyl transferase (*Hprt*) targeting system that we have used previously¹² applying 'Quick Knock-inTM' (GenOway) technology to generate genetically modified embryonic stem (ES) cells. This approach uses homologous recombination to target a single copy of a transgene (in this case the human IR) driven by a promoter (in this case the *Tie2* promoter) into the *Hprt* locus on the X chromosome.

As previously described,¹³ the model was developed with E15Tg2a (E14) cells derived from the strain 129P2/OlaHsd (12901a). Tissue-specific promoters including *Tie2*¹⁴ inserted into the *Hprt* locus maintain their expression properties. For detailed methods, see Supplemental Materials online.

Myeloid cell enumeration, isolation and transcriptional profiling

Peripheral blood mononuclear cells (PBMC) were isolated using density gradient centrifugation (Histopaque 1083; Sigma) of heparinised venous blood collected during terminal anaesthesia. 2×10^5 PBMC were used for labelling with an APC-conjugated CD11b antibody (AbD Serotec) or APC-conjugated isotype control, after blocking non-specific antibody binding with Fc receptor block (BD Biosciences). Monocytes were enumerated using an LSR-Fortessa cytometer (BD Biosciences) based on either typical light scatter properties, or separately based on CD11b expression, with normalisation to total mononuclear cell count (Supplemental Figure IA to IF). Remaining PBMC were incubated with CD11b microbeads (Miltenyi Biotec) prior to undergoing 2 rounds of magnetic purification using MS-columns (Miltenyi Biotec), achieving purity exceeding 90%. CD11b+ cells were immediately lysed using TRIzol reagent (Life Technologies), then total RNA isolated according the manufacturer's protocol. RNA was then cleaned (RNeasy MinElute; Qiagen), amplified and reverse transcribed to cDNA (QuantiTect; Qiagen), prior to qRT-PCR (LightCycler; Roche) using validated TaqMan probes (Life Technologies) for murine TNF- α , murine IL-1 β , murine IL-6, and human Insulin receptor. All expression was normalised to the cycle threshold of murine β -actin using the $2^{-\Delta\text{CT}}$ method. Human umbilical vein endothelial cells and HIRECO lung endothelial cells served as positive controls for human insulin receptor qRT-PCR.

Metabolic tests and plasma circulating levels of insulin, TNF alpha, IL6 and nitrite.

Blood was sampled from the lateral saphenous vein. Glucose and insulin tolerance tests were performed by blood sampling after an intraperitoneal (IP) injection of glucose (Sigma, 1 mg/g) or human recombinant insulin (0.75 unit/kg: Actrapid; Novo Nordisk, Bagsvaerd, Denmark) as previously described¹⁵. Glucose concentrations were determined in whole blood by a portable glucometer (Roche Diagnostics, 2 Burgess Hill, UK). Plasma insulin concentrations were determined by enzyme-linked immunoassay (Ultrasensitive mouse ELISA; CrystalChem, Downers Grove, IL, USA). Free fatty acids and triglycerides were measured in fasting plasma using colorimetric assays (AbCam). Plasma levels of TNF alpha, IL6 and nitrite were measured using colorimetric assays (AbCam).

In vivo blood pressure measurement. Systolic blood pressure was measured using tail-cuff plethysmography in conscious mice, as previously described.^{15,16} Mice were pre-warmed

for 10 minutes in a thermostatically controlled restrainer (CODA2 System, XBP1000; Kent Scientific). Three training sessions were performed during the week before measurements were taken. The mean of at least five separate recordings on three occasions was taken to calculate mean systolic blood pressure.

Studies of vasomotor function in aortic rings. Vasomotor function was assessed *ex-vivo* in aortic rings as previously described.¹⁵⁻¹⁷ Rings were mounted in an organ bath containing Krebs Henseleit buffer (composition [in mmol/L]: NaCl 119, KCl 4.7, KH₂PO₄ 1.18, NaHCO₃ 25, MgSO₄ 1.19, CaCl₂ 2.5, and glucose 11.0) gassed with 95% O₂/5% CO₂. Rings were equilibrated at a resting tension of 3g for 45min before the experiments. A cumulative dose-response to the constrictor phenylephrine (PE) (1nmol/L to 10 μ mol/L) was first performed. Relaxation responses to cumulative addition of acetylcholine (ACh) (1nmol/L-10 μ mol/l) and sodium nitroprusside (SNP) (0.1nmol/L-1 μ mol/l) were carried out. Insulin mediated vasorelaxation was assessed in 2 different ways: 1) direct vasorelaxation responses in response to incremental doses of Actrapid insulin (0.1-4mU/ml) in aortic segments pre-constricted maximally with PE. 2) Examining the effect of insulin to reduce PE mediated vasoconstriction as we previously reported.¹⁸ Relaxation responses are expressed as percentage decrement in pre-constricted tension. Bioavailable NO in aortic segments subjected to isometric tension was measured by recording the change in tension elicited by the non-selective endothelial NOS inhibitor, L-NMMA (0.1mmol/L) in aortic segments pre-constricted maximally with PE. (Percentage change calculated as percentage change from maximal constriction to PE after L-NMMA¹⁸). The effects of gp91ds-tat (50 μ mol/L for 30 min, GenScript) and MnTmPyP (10 μ mol/L for 30 min, Calbiochem) on aortic relaxation were examined, as previously reported.¹⁵

Nitric oxide synthase activity in endothelial cells. Upon activation, eNOS produces NO and L-citrulline in a stoichiometric reaction. The effect of insulin on eNOS activity in endothelial cells was determined by conversion of [14C]-L-arginine to [14C]-L-citrulline as we previously described.¹² Endothelial cells (1 x 10⁶ cells) were incubated at 37°C for 20 min in HEPES buffer pH 7.4 (in mmol/L): 10 HEPES, 145 NaCl, 5 KCl, 1 MgSO₄, 10 glucose, 1.5 CaCl₂ containing 0.25% BSA. 0.5 μ Ci/ml L-[14C] arginine (Amersham) was then added for 5 minutes and tissues stimulated with insulin (150nmol/L) for 45 min before the reaction was stopped with cold phosphate-buffered saline (PBS) containing 5 mmol/L L-arginine (Sigma Aldrich) and 4 mmol/L EDTA after which tissue was denatured in 95% ethanol. After evaporation, the soluble cellular components were dissolved in 20mmol/L HEPES-Na⁺ (pH 5.5) and applied to a well-equilibrated DOWEX (Na⁺-form) column (Sigma Aldrich). The L-[14C] citrulline content of the eluate was quantified by liquid scintillation counting and normalized against the total cellular protein used.

Immunoprecipitation of phosphorylated insulin receptor. Tyrosine phosphorylation of Insulin Receptor was quantified using Western blotting.¹⁷ Immunoprecipitation of protein for the quantification of receptors was achieved by incubating equal amounts of protein lysates (50 μ g) and 50 μ L of protein A-DynaBeads (Invitrogen) pre-coated with indicated rabbit anti-insulin receptor antibody for 20 minutes. After 3 rounds of washing with PBS-0.01%Tween-20, the beads were resuspended in 2x Laemmli loading buffer supplied with the NOVEX Gel Electrophoresis system. Cellular protein was separated by SDS-PAGE and blots were probed with a mouse Phospho-tyrosine 4G10 (Millipore), IR-beta (C-19) antibodies for receptor expression (Santa Cruz Biotechnologies). This experiment was performed after overnight serum-deprivation. Since basal levels would be decreased during this period, insulin-induced tyrosine phosphorylation of insulin receptor has been quantified and compared to vehicle control.

Cell lysis, Immunoblotting. Primary endothelial cells were cultured in 20% FCS-containing media for analysing basal protein levels. Cells were lysed in extraction buffer containing 50mM HEPES, 120mM NaCl, 1mM MgCl₂, 1mM CaCl₂, 10mM NaP₂O₇, 20mM NaF, 1mM

EDTA, 10% glycerol, 1% NP40, 2mM sodium orthovanadate, 0.5µg/ml leupeptin, 0.2mM PMSF, and 0.5µg/ml aprotinin. Insulin-stimulated endothelial cells were serum-deprived overnight with 1% FCS-containing endothelial cell media before stimulation and harvesting in lysis buffer for western blot analysis. Cell extracts were sonicated in an ice-bath and centrifuged for 15 minutes at 13000 rpm, before protein measurements were carried out by BCA assay (Pierce Protein Quantification Kit) using the supernatant. Equal amounts of cellular protein were resolved on SDS polyacrylamide gels (Invitrogen) and transferred to polyvinylidene difluoride membranes and immunoblotted with appropriate antibodies (for details see Supplemental Material). The assays are run on the same blot for both wild type and transgenic mice, whenever possible to fit all experimental conditions onto one gel, thereby negating issues with exposure time. Our approach using the Syngene densitometry (Syngene Gel Documentation) system also avoids issues with exposure time and blotting efficiency. Wherever stimulation has been carried out after overnight serum-deprivation, the result has been calculated as percentage of vehicle control.

Assessment of superoxide generation

Lucigenin enhanced chemiluminescence. We used lucigenin (5µmol/L)-enhanced chemiluminescence to measure NAD(P)H-dependent superoxide production in pulmonary endothelial cells, as previously described.⁹ All experiments were performed in triplicate. Pulmonary endothelial cell monolayer was trypsinized and re-suspended in PBS containing 5% FCS, 0.5% BSA and 50µmol/L gp91ds-tat (gp91; GenScript) or scrambled peptide (Scr; GenScript) and incubated at 37°C for 30 min. Luminescence was then measured upon addition of a non-redox cycling concentration of lucigenin (5µM) and NADPH (100µmol/L), using an autodispenser (VarioSkan 96-well microplate luminometer, Thermo Scientific). Wortmannin (WM; 50 nanomol/L, Calbiochem) and LY294002 (LY; 25nmol/L, Calbiochem) was used to inhibit PI3-kinase and MK-2206 (MK; 10 micromol/L, Calbiochem) to inhibit Akt in pulmonary endothelial cells to study the role of PI3-kinase and Akt in NADPH oxidase-induced superoxide production. Where wortmannin, LY294002 or MK-2206 were used for the measurement of reactive oxygen species production, endothelial cell suspension was prepared from both wild type and hIRECO mice in equal cell concentration. The inhibitors were incubated for 30 minutes before measuring free radical generation. Data presented as percent decrease against non-inhibited cells.

High performance liquid chromatographic measurement of conversion of dihydroethidium to oxyethidium. In order to measure Nox2 dependent aortic superoxide production, we used high performance liquid chromatography (HPLC)-based detection of the oxidation products of dihydroethidium (DHE, Invitrogen), i.e. 2-hydroxyethidine (EOH) and ethidium (E), as previously described²⁵ in aortic rings from hIRECO and wild type mice exposed to the nox2 inhibitor gp91dstat (for detailed methods, see Supplemental Material).

Amplex red assay for hydrogen peroxide in aorta. H₂O₂, the downstream dismutation product of superoxide, was measured using an Amplex® Red Hydrogen Peroxide/Peroxidase Assay Kit (Molecular Probes, Life Technologies) according to the manufacturer's protocol (for detailed methods, see Supplemental Material).

Gene expression. mRNA was isolated using a commercial kit (Sigma Aldrich), and the levels of *eNOS*, *Nox2*, *Nox4*, *SOD*, *catalase*, *ve-cadherin*, *IL6*, *TNF alpha* and *IR* mRNA quantified using real-time quantitative PCR (SYBR Green-based or Taqman Probe assay in AB Systems 7900HT machine (Supplemental Table 1)¹⁵. A range of housekeeping genes were screened for variability and stability. Non-specific primers and those specific for human and mouse *IR* were designed and validated in human umbilical vein endothelial cells and mouse pulmonary endothelial cells (Supplemental Table I).

Endothelial cell isolation and culture. Primary endothelial cells were isolated from lungs by immunoselection (Supplemental Figure IIIB) with CD146-antibody-coated magnetic beads

(Miltenyi Biotechnology) as previously reported.¹⁷ (for detailed methods, see Supplemental Material)

Exposure of endothelial cells to flow-mediated shear stress. Pulmonary endothelial cells were seeded onto fibronectin-coated 6-well plates. Once confluent, monolayers were placed onto an orbital rotating platform (Grant Instruments) housed inside the incubator.¹⁹ The radius of orbit of the orbital shaker was 10mm and the rotation rate was set to 210rpm for 10 minutes, which caused swirling of the culture medium over the cell surface volume. The movement of fluid due to orbital motion represents a free surface flow at the liquid-air interface at 12 dyne/cm².

Chronic pharmacological inhibition of NADPH oxidase. To examine the effect of inhibition of *Nox2* NADPH oxidase on endothelial cell function in hIRECO mice, we performed chronic treatment studies using the peptidic *Nox2* inhibitor, gp91ds-tat. hIRECO mice were anaesthetised and osmotic mini-pumps (Alzet 2004) containing gp91ds-tat or control scrambled peptide implanted, as previously reported.¹⁵ The pump delivered 0.25uL of drug per hour for 28 days. The concentration of the scrambled and gp91ds-tat peptide was adjusted (50mg/ml) to deliver 10mg/kg/day. Animals were sacrificed after 28 days and organ bath experiments were carried out to assess vasomotor function.

siRNA-mediated knockdown of Nox2 NADPH oxidase and proline-rich tyrosine kinase. Silencing of *PYK2* and *Nox2* NADPH oxidase gene expression in pulmonary endothelial cells was carried out by transfection of mouse siRNA duplexes (Stealth RNAi, Invitrogen) with Lipofectamine RNAiMax Transfection Reagent (Invitrogen) exactly according to manufacturer's established protocol and as we previously, reported.¹⁵ Scrambled siRNA was used as negative control (Invitrogen) for transfection. Briefly, isolated pulmonary endothelial cells from lung tissues were rendered 70% confluent and transfected with 25pmol siRNA for 72 hours before cell lysates were prepared for quantitative RT-PCR and western blotting analysis.

Quantification and characterisation of atherosclerosis. In order to study the effects of endothelial IR over-expression on the development of atherosclerosis, we crossbred hIRECO mice with mice holoinsufficient for ApoE (*ApoE*^{-/-}). Mice (*ApoE*^{-/-} and *ApoE*^{-/-}/hIRECO) were fed a western diet (21% fat from lard supplemented with 0.15% wt/wt cholesterol, #829100, SDS, Witham, Essex, UK) for 12 weeks from 4 weeks of age to induce atherosclerosis.²⁰ Mice were surgically anaesthetised by intraperitoneal injection of sodium pentobarbitone before thorough terminal exsanguination by arterial perfusion via the abdominal aorta with PBS at a constant pressure of 100mmHg with outflow through the severed jugular veins. This was followed by constant pressure perfusion *in-situ* with 10% formalin. The heart was removed to study the aortic sinus. In other animals, the thoracic and abdominal aorta was dissected to allow *en face* quantification of plaque development.

Plaque quantification in *en face* sections of aorta. For *en face* analysis, aortas were analysed, as previously described.^{16,20} Briefly, aortas were removed, fixed in PBS-buffered 4% formalin, cut longitudinally, stained with Oil Red O, and photographed (Olympus digital camera QICAM) under dissection microscope (Olympus SZ61). Percentage coverage of plaque area was measured using Image-Pro Plus 6.0 (Media Cybernetic, Bethesda, MD) software.

Statistics. Results are expressed as mean±SEM. Comparisons within groups were made using paired Student's t-tests and between groups using unpaired Student's t tests, as appropriate; where repeated t-tests were performed a Bonferroni correction was applied. P<0.05 was considered statistically significant.

Results

Generation and characterisation of transgenic mice over-expressing the human insulin receptor in the endothelium. To examine the effect of enhancing insulin sensitivity in the endothelium, we generated a novel transgenic mouse over-expressing the human type A insulin receptor directed to the endothelium under control of the *Tie2* promoter-enhancer (henceforth, described as human insulin receptor endothelial cell over expressing mice, hIRECO, Supplemental Figure IA-D). hIRECO were born with the same frequency as wild type littermates, and there was no difference in growth (Figure 1A, left) or organ weight, measured at 12 weeks of age (Figure 1A, right) between hIRECO and wild type littermates (WT). We quantified levels of human and native (mouse) insulin receptor (IR) mRNA expression in organs with differing vascularity (heart, lung, spleen). Human IR mRNA expression in hIRECO recapitulated the pattern for native IR seen in wild type mice (Figure 1B). There was no difference in mRNA expression of endogenous insulin receptor between hIRECO and wild type (Figure 1C). There was no human IR mRNA detectable in endothelial cells from wild type mice or non-endothelial cells from hIRECO (Figure 1D). Non-endothelial cells did not express the endothelial-specific marker, ve-cadherin in contrast to endothelial cells (Figure 1E). mRNA expression of mouse IR also remained unchanged in the isolated EC (Figure 1F). Total IR protein expression was significantly increased in hIRECO endothelial cells compared to wild-type littermates (Figure 1G). Some studies have suggested that the *Tie2* promoter-enhancer drives the expression in myeloid cells.²¹ In order to examine this possibility, we isolated circulating CD11b⁺ myeloid cells from hIRECO and wild type littermates, as previously described.²² There was no difference in total circulating CD11b⁺ or monocyte count (Supplemental Figure IIA-C), gene expression of TNF-alpha, IL-1beta and IL-6 in hIRECO CD11b⁺ cells (Supplemental Figure IID-F) or concentrations of the circulating inflammatory cytokines TNF-alpha and IL-6 in hIRECO (Supplemental Figure IIIC and D) compared to wild type littermates. We could not detect human IR mRNA in monocytes from hIRECO.

Enhanced endothelial cell insulin sensitivity in hIRECO mice. Consistent with enhanced insulin action at the insulin receptor signalling node, basal and insulin-stimulated levels of tyrosine phosphorylated IR were substantially higher in endothelial cells from hIRECO compared to their wild type littermates (Figure 2A). Basal serine-473 phosphorylation of Akt in endothelial cells from hIRECO was markedly enhanced (Figure 2B, right) as was basal eNOS serine-1177 (Figure 2B, left). In dose-response experiments, Akt phosphorylation in response to insulin was also significantly enhanced in hIRECO endothelial cells (Figure 2C).

hIRECO mice have normal glucose tolerance and blood pressure and elevated plasma nitrite. Over-expression of the IR in the endothelium had no effect on fasting glucose, (Figure 3A) fasting insulin levels (Figure 3B) or blood pressure levels at the age of 3 months (Figure 3C). hIRECO had similar responses in glucose tolerance tests (Figure 3D) and insulin tolerance tests (Figure 3E) to wild type littermates. Plasma triglycerides (Figure 3F) and free fatty acid levels (Figure 3G) were not different between hIRECO and wild type littermates. Consistent with increased basal eNOS serine phosphorylation, plasma nitrite was also increased (Supplemental Figure IIIE).

hIRECO mice have reduced NO availability. We examined the effect of excessive insulin signalling on aortic vasomotor responses in an organ bath. Aortic rings from hIRECO mice had blunted responses to the endothelium- and NO-dependent vasodilator, acetylcholine (ACh, Figure 4A). Vasoconstriction to phenylephrine (PE) remained unchanged in hIRECO compared to wild type littermates (Figure 4B), as did vasorelaxation in response to the endothelium-independent vasodilator sodium nitroprusside (SNP, Figure 4C). Basal NO production in response to isometric tension assessed by measuring the constrictor response to the NO synthase inhibitor L-NMMA was reduced in hIRECO mice (Figure 4D, Supplemental Figure IV B). In aortic rings from hIRECO animals we assessed insulin-mediated NO-dependent vasorelaxation followed by 2 methods. Insulin pre-treatment blunts

phenylephrine-induced vasoconstriction in an NO- and endothelium-dependent fashion.¹⁸ We demonstrated that this vasodilatory response to insulin was blunted in hIRECO mice aortae (Figure 4E), as was acute vasorelaxation of phenylephrine pre-constricted aortic rings in response to varying doses of insulin (Figure 4F; left). Moreover, L-NMMA significantly blunted insulin-mediated vasodilatation (Figure 4F; right), demonstrating that insulin-mediated vasodilation is NO-dependent. There was also a significant reduction in eNOS activity in response to insulin in hIRECO endothelial cells compared to endothelial cells from wild type littermates (Figure 4G). Therefore, increased expression of the insulin receptor in the endothelium leads to resistance to insulin downstream of Akt. In response to chemical cues (e.g. insulin) and mechanical stimuli (e.g. shear stress), Akt is activated leading to serine-1177 phosphorylation of eNOS to stimulate generation of NO.^{23,24} Therefore, we assessed if phosphorylation of Akt and eNOS were impaired in the hIRECO endothelial cells; leading to decreased NO and vasodilation observed in these hIRECO mice. We demonstrated that shear stress-mediated serine phosphorylation of Akt was similar between both groups of mice (Figure 4H). Interestingly, shear stress-mediated serine phosphorylation of eNOS (Figure 4I) was blunted in hIRECO when compared to wild type littermates.

Nox2 NADPH oxidase and excess superoxide in hIRECO mice. Decreased endothelium-dependent vasorelaxation and reduced NO bioavailability could be mediated by increased superoxide generation.¹⁵ In order to examine the possibility that the underlying mechanism of the blunted acetylcholine responses in hIRECO mice is at least, in part due to excess superoxide, we exposed aortic rings from hIRECO to the superoxide dismutase mimetic, Mn(III) tetrakis (1-methyl-4-pyridyl) porphyrin pentachloride (MnTmPyP) before performing dose-response studies to acetylcholine (Figure 5A). Consistent with excessive generation of superoxide, the maximal relaxation of rings from hIRECO mice in response to acetylcholine in the presence of MnTmPyP was significantly restored to normal wild type level. We have previously demonstrated that mice with whole body⁸ and endothelium-specific insulin resistance¹⁵ have excess generation of superoxide as a result of increased Nox2 NADPH oxidase activity. In order to examine the possibility of this underlying mechanism in mice with enhanced endothelial insulin signalling, we treated aortic rings from hIRECO mice with gp91ds-tat, a Nox2 specific NADPH oxidase inhibitor and assessed the response to acetylcholine. Consistent with this hypothesis, gp91ds-tat significantly increased the maximal response to acetylcholine of aortae from hIRECO mice (Figure 5B). We investigated the role of superoxide in endothelial function by direct measurement of superoxide release in isolated endothelial cells, using NADPH-dependent lucigenin-enhanced chemiluminescence assay, confirming the effects seen the organ bath studies. hIRECO endothelial cells demonstrated a 1.5-fold increase in superoxide release (Figure 5C). This finding was associated with a significant increase in Nox2 protein expression (Figure 5D) in hIRECO endothelial cells. The basal increase in superoxide production in hIRECO endothelial cells was reduced to wild type levels, in the presence of gp91ds-tat (Figure 5E, left) as well as in hIRECO aorta measured using HPLC (Figure 5E, centre) indicating that Nox2 NADPH oxidase was the principal source of the excess superoxide. Amplex Red quantification of hydrogen peroxide demonstrated marked increase in hydrogen peroxide release in hIRECO endothelial cells (Figure 5E, right). To examine further the effect of chronic pharmacological inhibition of Nox2 NADPH oxidase, we administered gp91ds-tat to hIRECO mice via osmotic mini-pump for 28 days, as we described recently.¹⁵ Chronic treatment with gp91ds-tat had no effect on body mass (Figure 5F), organ weight (Supplemental Figure IV A), glucose (Figure 5G:left) and insulin tolerance tests in hIRECO mice (Figure 5G:center). To examine the effect of chronic *in vivo* pharmacological inhibition of NADPH oxidase on endothelium-dependent vasomotor responses, we studied aortic rings from hIRECO mice after treatment with gp91ds-tat or scrambled peptide to examine acetylcholine-induced vasorelaxation *ex vivo*. Gp91ds-tat significantly enhanced (albeit to a small extent) maximal acetylcholine-induced aortic relaxation compared to scrambled peptide (Figure 5H). Chronic treatment with gp91ds-tat had no effect on SNP-mediated vasorelaxation in hIRECO (data not shown) indicative of preservation of responses in vascular smooth muscle.

In order to determine whether the negative effects of excessive endothelial insulin signalling is a consequence of alteration of expression of various protective or compensatory antioxidant enzymes, quantitative real-time polymerase chain reaction experiments were performed in endothelial cells. hIRECO mice had no difference in expression of superoxide dismutase (SOD) 1, SOD2, SOD3, or catalase. (Supplemental Figure IIIA).

Insulin-stimulated superoxide generation in hIRECO mice. We next examined the involvement of the critical signalling node PI3-kinase in generation of the excessive superoxide release seen in hIRECO mice using the PI3-kinase inhibitors, Wortmannin and LY294002.²⁶ Wortmannin inhibited NADPH-dependent superoxide production assessed using lucigenin-enhanced chemiluminescence (Figure 6A), as did an alternative PI3-kinase inhibitor LY294002 (Figure 6B), demonstrating that the PI3-kinase signalling node is potentially important for the increased endothelial superoxide production in hIRECO mice. Previous studies have suggested that downstream of PI3-kinase increased Akt activation may lead to increased oxidative stress.^{27,28} Since we found that hIRECO had increased Akt activation, we treated hIRECO endothelial cells with the allosteric Akt inhibitor, MK-2206.²⁹ MK-2206 reduced superoxide generation from hIRECO endothelial cells (Figure 6C). We examined further, whether insulin-stimulated superoxide generation in endothelial cells from hIRECO is mediated via AKT and Nox2 activation. Therefore, we assessed the effects of Akt and Nox2 blockers, MK-2206 or gp91ds-tat, respectively. Insulin did not stimulate a detectable increase in superoxide in wild type endothelial cells. Insulin, however did stimulate an increase in superoxide production in hIRECO endothelial cells (Figure 6D). This excess generation of superoxide in response to insulin was blunted by the Akt inhibitor MK-2206 (Figure 6D) and the Nox2 inhibitor gp91ds-tat (Figure 6D) demonstrating that the insulin-stimulated increment in superoxide was Akt and Nox2 dependent.

Role of eNOS tyrosine phosphorylation in endothelial dysfunction in hIRECO mice. Previous studies have demonstrated that insulin, by increasing the expression of proline rich tyrosine kinase 2 (PYK2), may lead to phosphorylation of eNOS on tyrosine residues which inhibit eNOS activity.¹¹ To examine this possibility, we measured levels of tyrosine-657 phosphorylated eNOS in endothelial cells from hIRECO. We found that phosphorylation of the inhibitory residue Tyr657 was significantly increased in hIRECO compared to wild type littermates (Figure 6E, left) and inhibition of NOX2 by gp91ds-tat significantly reversed this effect (Figure 6E, right). Moreover, expression of PYK2 was also increased (Figure 6F) and the expression of phosphorylated PYK2 was similar when comparing hIRECO to wild type littermates (data not shown). To further examine the role of PYK2 in endothelial dysfunction in hIRECO using siRNA in isolated endothelial cells, we reduced PYK2 expression by approximately 50 percent (Figure 6G). In siRNA treated cells, we assessed eNOS activity and performed the L-arginine to L-citrulline conversion assay in the presence of insulin and eNOS phosphorylation in response to shear stress. Both insulin-stimulated eNOS activity (Figure 6H) and shear stress-mediated eNOS serine-phosphorylation (Figure 6I) were significantly increased in hIRECO cells with reduced PYK2.

Examining crosstalk between Nox2 and PYK2. In order to examine the possibility of crosstalk between Nox2 and PYK2, we performed siRNA experiments knocking down either Nox2 or PYK2. These experiments revealed an intriguing, yet previously unrecognised feed-forward loop. Chronic reduction of Nox2 activity with gp91 ds-tat and inhibiting Akt with MK-2206 reduced PYK2 expression in the hIRECO endothelial cells (Figure 7A). MK-2206 and gp91ds-tat reduced PYK2 expression revealing a new signalling circuit linked to enhanced insulin signalling including Akt, Nox2 and PYK2 which conspire to reduce basal and stimulated NO bioactivity. To further examine this interaction in hIRECO mice, we used siRNA to knockdown Nox2; this led to reduced PYK2 expression (Figure 7B), indicative of superoxide-mediated regulation of PYK2 expression in hIRECO mice. Knockdown of PYK2 in hIRECO endothelial cells with siRNA significantly reduced NOX2 expression (Figure 7C) and also improved eNOS phosphorylation in the presence of insulin (Figure 7D). However,

knockdown of NOX2 failed to reverse the decrease in insulin-stimulated eNOS phosphorylation (Figure 7D), suggesting that the reduction of insulin-stimulated eNOS phosphorylation is mediated via increases in PYK2 activity and not directly through Nox2 activation.

Over-expression of insulin receptor in the endothelium leads to accelerated atherosclerosis. In order to examine the effect of over-expression of insulin receptor in the endothelium on the development of advanced atherosclerosis, we crossed pro-atherogenic ApoE^{-/-} mice with hIRECO to generate ApoE^{-/-}/hIRECO. ApoE^{-/-}/hIRECO and ApoE^{-/-} littermates were fed a high cholesterol western diet for 12 weeks from 8 weeks of age. After 12 weeks feeding, body weights were similar in ApoE^{-/-}/hIRECO and ApoE^{-/-} littermates (Figure 8A). Systolic blood pressure (Figure 8B), plasma cholesterol (Figure 8C) and triglyceride levels (Figure 8D) were no different in ApoE^{-/-}/hIRECO compared to ApoE^{-/-}. Fasting glucose (Figure 8E) was similar between ApoE^{-/-}/hIRECO and ApoE^{-/-}. Glucose homeostasis assessed in glucose tolerance (Figure 8F) and insulin tolerance tests were comparable between ApoE^{-/-}/hIRECO and ApoE^{-/-} (Figure 8G). In contrast, ApoE^{-/-}/hIRECO demonstrated a significant increase in the development of atherosclerosis in the whole aorta (Figure 8H) and also at the level of the aortic sinus (Figure 8I). We describe here a novel proatherosclerotic signalling loop whereby increased endothelial cell insulin sensitivity leads to overactivation of NOX2, generating excess superoxide anion and thereby, decreasing nitric oxide availability. Activation of NOX2 in turn, leads to increased PYK2 expression and eNOS tyrosine phosphorylation. This effect leads to a further decrease in NO availability and enhanced atherogenesis (Figure 8J).

Discussion

Despite intensive efforts to prevent the adverse effects of type 2 diabetes on cardiovascular morbidity and mortality, the presence of insulin resistant type 2 diabetes substantially increases the risk of developing atherosclerosis-related vascular disease.⁴ The presence of type 2 diabetes also significantly worsens the prognosis of most of the adverse sequelae of atherosclerotic arterial disease including; myocardial infarction,³⁰ left ventricular dysfunction³¹ and peripheral vascular disease.³² Improving our understanding of mechanisms linking accelerated atherosclerosis and insulin signalling is thus of critical importance. Here, we describe the phenotype of a novel transgenic mouse with endothelium-targeted over-expression of the human IR, generated to investigate the local and systemic consequences of prolonged enhancement of insulin sensitivity in the endothelium. This is the first description of a manipulation of the insulin signalling pathway leading to specific enhancement of insulin action in the endothelium; a model of particular relevance as insulin sensitisation is a strategy actively pursued to treat patients suffering from the cardiovascular complications of type 2 diabetes.³³ Here, we show that increased insulin sensitivity specifically in the endothelium, (a model of excess insulin action independent of systemic influences) at the most proximal node in its signalling pathway has relevant pathophysiological effects on its downstream targets.

The major finding of our study is that specific and prolonged enhancement of insulin signalling in the endothelium *in vivo* establishes a positive proatherosclerotic signalling loop around the Akt signalling node, involving: the protein kinase Akt, the superoxide generating Nox2 NADPH oxidase, the proline rich non-receptor tyrosine kinase, PYK2 and the endothelial NO synthase isoform. This circuit impacts negatively on NO actions in 2 ways: 1) by increasing Nox2 NADPH oxidase-derived superoxide which reacts with NO to reduce its availability. 2) by increasing expression of PYK2 which reduces NO production by tyrosine phosphorylation of eNOS, a modification shown to attenuate the activity of the enzyme. The convergence of these adverse pathways leads to a significant reduction in a range of downstream actions, fundamental to the homeostatic function of NO which allied to excess concentrations of endothelial cell-derived superoxide leads to a proatherosclerotic vascular environment. Indeed, consistent with this, hIRECO mice crossed onto an atherosclerosis-prone Apolipoprotein E deficient background developed significantly more atherosclerosis at the level of the aortic sinus and whole aorta compared to Apolipoprotein E-deficient littermates. Interestingly we did not see an increase in systolic blood pressure in hIRECO mice consistent with our findings in mice with endothelial specific insulin resistance due to expression of a dominant negative insulin receptor.⁹ These findings may reflect the relative importance of insulin receptors in arteries of different size. We also saw no effect on glucose homeostasis in hIRECO mice similar to mice with endothelial specific insulin resistance due to expression of a dominant negative insulin receptor and unlike mice with endothelial cell specific deletion of insulin receptor substrate-2 suggesting that the effect of endothelial cell insulin sensitivity on whole body glucose homeostasis is complex and may depend on the signalling node involved.³⁴

Insulin activates its intracellular signalling pathway by binding to and activating its tyrosine kinase receptor, which leads to activation of IR substrates (IRS). Downstream of IRS is phosphatidylinositol 3-kinase (PI3-K) which activates the serine/threonine kinase Akt.³⁵ Upon insulin stimulation, Akt is phosphorylated by phosphoinositide dependent kinase-1 and the mechanistic target of rapamycin complex-2 to yield a fully activated kinase, which phosphorylates eNOS to increase NO synthesis in response to a range of cues, including mechanical shear stress and insulin.^{23,24} While deletion of Akt has been shown to promote the development of atherosclerosis³⁶ and short-term enhancement of Akt activity has been shown to increase NO availability,³⁷ unrestrained Akt activity may contribute to the development of atherosclerosis²⁸ and in the setting of obesity contribute to the development of oxidative stress.²⁷ Here, we demonstrate that endothelial cell over-expression of IR increases basal and insulin stimulated activation of Akt, which increases the activity and

expression of the superoxide generating enzyme Nox2 NADPH oxidase. While a link between PI3-K/Akt and NADPH oxidase has been proposed,^{38,39} this is the first study to unequivocally demonstrate a direct pathway between enhanced insulin sensitivity, PI3-K, Akt activation and Nox2 NADPH oxidase activity. During normal physiology, the NADPH oxidases generate low levels of reactive oxygen species in a highly regulated fashion for use in redox-dependent signalling.⁴⁰ When the generation of reactive oxygen species exceeds their homeostatic threshold, a range of disorders of the human cardiovascular system may ensue.⁴¹ Enhancing insulin sensitivity in the endothelium not only increased basal superoxide generation, but also led to the ability of endothelial cells from hIRECO to generate superoxide in response to insulin, unlike cells from wild type mice. This insulin-mediated superoxide release was blunted by specific inhibitors of Nox2 and Akt.

We also demonstrated increased endothelial cell expression of the cytoplasmic tyrosine kinase PYK2 in hIRECO mice. PYK2 is activated in response to a range of stimuli and is thought to be important in coupling several receptors with downstream effectors.⁴² Elegant work by Fisslthaler *et al.*¹¹ has shown that insulin and shear stress increase expression levels of PYK2 which in turn phosphorylates a tyrosine residue on eNOS, which leads to inhibition of enzyme activity and reduced NO generation. This effect, which was shown to be independent of reactive oxygen species and dependent on absolute expression levels of PYK2, has emerged as a potentially important regulator of NO generation. Here, we show in an *in vivo* model that selective enhancement of insulin sensitivity in the endothelium leads to increased expression of PYK2 and a concurrent increase in tyrosine phosphorylation of eNOS (Figure 8J). Inhibition of PYK2 reversed the detrimental effect of excess insulin signalling on insulin and shear stress-induced eNOS activation. We demonstrated no difference in phosphorylated PYK2 in hIRECO endothelial cells. However, consistent with the work of Fisslthaler *et al.*¹¹ an increase in the absolute levels of PYK2 expression was sufficient to inhibit eNOS in our system. We took this further by demonstrating that pharmacological blockade of Akt reduced the expression of PYK2 and we also demonstrated for the first time that Nox2-derived superoxide increases the expression of PYK2. This concomitant increase in PYK2 expression and downstream phosphorylation of eNOS at tyrosine residue 657 reduces eNOS activity and NO generation (Figure 8J). While other residues on eNOS could be phosphorylated and inhibit enzyme activity¹¹ our data clearly demonstrate a key role for tyrosine residue 657 in insulin mediated adverse effects on eNOS activity. Consistent with our findings in mice with whole body insulin resistance we demonstrated an increase in basal serine phosphorylated eNOS⁹ which may itself limit further increments in eNOS activation in response to different stimuli. While our gain of function transgenic model generated using the hprt approach does circumvent some of the problems with standard transgenic models, it will be important in the future to generate and examine complementary gene-modified models with targeted knockout of key downstream proteins to enhance insulin signalling at different signalling nodes in the endothelium.

Our data provides evidence of the integration of two discrete but interrelated signalling pathways, impacting unfavourably on NO availability. Enhancing insulin sensitivity in the endothelium led to excess generation of superoxide, which in a range of complementary assays we showed to be Nox2 NADPH oxidase-dependent. Via increased expression of PYK2, enhancing insulin sensitivity led to attenuation of eNOS activity in response to insulin and shear stress. At the centre of this lies Akt, driving the expression of both Nox2 and PYK2. It is important to note that type 2 diabetes is a progressive disorder and insulin hypersecretion can occur in healthy humans well before the onset of insulin resistant type 2 diabetes.⁴³ Indeed, hyperinsulinaemia is a strong independent predictor of the development of atherosclerosis in individuals free from diabetes.⁴⁴ We have demonstrated that metabolic insulin resistance may precede vascular insulin resistance.⁴⁵ Whether, individuals at early stages of the disease before the onset of hyperglycaemia or indeed individuals with type 1 diabetes treated with high dose of insulin have evidence of the pro-atherosclerotic signalling circuit in the endothelium demonstrated here warrants investigation.

Acknowledgements. This work was supported by British Heart Foundation programme grant RG/09/010. We would like to thank Luke Brewin, Nuffield Research Foundation scholar, as well as Joseph Turner, Aneesa Razaq and Kar Yeun Tang from the University of Huddersfield-LICAMM Work Placement Programme, for their invaluable technical support.

Sources of Funding. This work was supported by British Heart Foundation programme grant RG/09/010.

Disclosures: Authors disclose no conflict of interest.

Supplemental Material

Supplemental Figures include Detailed Methods, four figures, one table and Supplemental References can be found with this article Supplemental Materials.

References

1. Shaw JE, Sicree RA, Zimmet PZ. Global estimates of the prevalence of diabetes for 2010 and 2030. *Diabetes Res. Clin. Pract.* 2010;87:4-14.
2. Soccio RE, Chen ER, Lazar MA. Thiazolidinediones and the promise of insulin sensitisation in type 2 diabetes. *Cell Metabolism.* 2014;20:573-591.
3. Samuel VT, Shulman GI. Mechanisms for insulin resistance: common threads and missing links. *Cell.* 2012;148:852-871.
4. Booth GL, Kapral MK, Fung K, Tu JV. Relation between age and cardiovascular disease in men and women with diabetes compared with non-diabetic people: a population based retrospective cohort study. *Lancet.* 2006;368:29-36.
5. Murad F. Shattuck Lecture. Nitric oxide and cyclic GMP in cell signaling and drug development. *N Engl J Med.* 2006;355:2003-2011.
6. Muniyappa R, Montagnani M, Koh KK, Quon MJ. Cardiovascular actions of insulin. *Endocr Rev.* 2007 ;28:463-491.
7. Kim JA, Montagnani M, Koh KK, Quon MJ. Reciprocal relationships between insulin resistance and endothelial dysfunction: molecular and pathophysiological mechanisms. *Circulation.* 2006;113:1888-1904.
8. Duncan ER, Walker SJ, Ezzat VA, Wheatcroft SB, Li JM, Shah AM, and Kearney MT. Accelerated endothelial dysfunction in mild prediabetic insulin resistance: the early role of reactive oxygen species. *Am J Physiol Endocrinol Metab.*2007;293:E1311-1319.
9. Duncan ER, Crossey PA, Walker S, Anilkumar N, Poston L, Douglas G, Ezzat VA, Wheatcroft SB, Shah AM, Kearney MT. Effect of endothelium specific insulin resistance on endothelial function in vivo. *Diabetes.* 2008;57:3307-3314.
10. Rask-Madsen C, Li Q, Freund B, et al. Loss of insulin signalling in vascular endothelial cells accelerates atherosclerosis in apolipoprotein E null mice. *Cell Metabolism.* 2010 ;11: 379-389.
11. Fisslthaler B, Loot AE, Mohamed A, Busse R, Fleming I. Inhibition of endothelial nitric oxide synthase activity by proline-rich tyrosine kinase 2 in response to fluid shear stress and insulin. *Circ Res.* 2008;102:1520-1528.
12. Imrie H, Viswambharan H, Sukumar P et al. Novel role of the IGF-1 receptor in endothelial function and repair: studies in endothelium-targeted IGF-1 receptor transgenic mice. *Diabetes.* 2012;61:2359-2368.
13. Minami T, Kuivenhoven JA, Evans V, Kodama T, Rosenberg RD, Aird WC. Ets motifs are necessary for endothelial cell-specific expression of a 723-bp Tie-2 promoter/enhancer in Hprt targeted transgenic mice. *Arterioscler Thromb Vasc Biol.* 2003;23:2041-2047.
14. Guillot PV, Liu L, Kuivenhoven JA, Guan J, Rosenberg RD, Aird WC. Targeting of human eNOS promoter to the Hprt locus of mice leads to tissue-restricted transgene expression. *Physiol Genomics.* 2000;2:77-83.

15. Sukumar P, Viswambharan H, Imrie H, et al.. Nox 2 NADPH oxidase has a critical role in insulin resistance-related endothelial cell dysfunction. *Diabetes*. 2013;2130-2134.
16. Rajwani A, Ezzat VA, Smith J. et al. Increasing circulating IGFBP1 levels improves insulin-sensitivity, promotes nitric oxide production, lowers blood pressure and protects against atherosclerosis. *Diabetes*. 2012;61:915-24.
17. Abbas A, Imrie H, Viswambharan H, et al. The Insulin-Like Growth Factor-1 Receptor Is a Negative Regulator of Nitric Oxide Bioavailability and Insulin Sensitivity in the Endothelium. *Diabetes*. 2011;60:2169-2178.
18. Wheatcroft SB, Shah AM, Li JM, Duncan E, Noronha BT, Crossey PA, Kearney, MT. Preserved glucoregulation but attenuation of the vascular actions of insulin in mice heterozygous for knockout of the insulin receptor. *Diabetes*. 2004;53:2645-2652.
19. Li J, Hou B, Tumova S, et al. Piezo1 integration of vascular architecture with physiological force. *Nature*. 2014;515:279-282.
20. Gage MC, Yuldasheva NY, Viswambharan H, Sukumar P, Cubbon RM, Galloway S, Imrie H, Skromna A, Smith J, Jackson CL, Kearney MT, Wheatcroft SB. Endothelial Specific Insulin Resistance Promotes the Development of Atherosclerosis in areas with disturbed flow patterns: a role for reactive oxygen species. *Atherosclerosis*. 2013;230:131-139.
21. Murdoch C, Tazzyman S, Webster S, Lewis CE. Expression of Tie-2 by human monocytes and their responses to angiopoietin-2. *J. Immunol*. 2007;178:7405–7411.
22. Yuldasheva NY, Rashid ST, Haywood NJ. et al. Haploinsufficiency of the insulin-like growth factor-1 receptor enhances endothelial repair and favourably modifies angiogenic progenitor cell phenotype. *Arterioscler. Thromb. Vasc Biol*. 2014;34:2051-2058.
23. Fulton D, Gratton JP, McCabe TJ, Fontana J, Fujio Y, Walsh K, Franke TF, Papetropoulos A, Sessa WC. Regulation of endothelium-derived nitric oxide production by the protein kinase Akt. *Nature*. 1999;399:597–601.
24. Dimmeler S, Fleming, Fisslthaler B, Herman C, Busse R, and Zeiher AM. Activation of nitric oxide synthase in endothelial cells by Akt-dependent phosphorylation. *Nature* .2009;399:601-605.
25. Laurindo FR, Fernandes DC, Santos CX. Assessment of superoxide production and NADPH oxidase activity by HPLC analysis of dihydroethidium oxidation products. *Methods Enzymol*. 2008; 441: 237-260.
26. Dimmeler S, Assmus B, Hermann C, Haendeler B, and Zeiher AM. Fluid Shear Stress Stimulates Phosphorylation of Akt in Human endothelial Cells Involvement in Suppression of Apoptosis. *Circ Res* 1998;83:334-341.
27. Wang CY, Kim HH, Hiroi Y, Sawada N, Salomone S, Benjamin LE, Walsh K, Moskowitz M,A., Liao JK. Obesity increases vascular senescence and susceptibility to ischemic injury through chronic activation of Akt and mTOR. *Sci Signal*. 2009; 2, (62):ra11.

28. Kerr BA, Ma L, West XZ, Ding L, Malinin NL, Weber ME, Tischenko M, Goc A, Somanath PR, Penn MS, Podrez EA, Byzova TV. Interference with akt signaling protects against myocardial infarction and death by limiting the consequences of oxidative stress. *Sci Signal* 2013; 6:287 ra67.
29. McGuane JT, Julianna E, Debrah JE, Sautina L, Jarajapu YPR, Novak J, Rubin JP, Grant MB, Segal M, Conrad KP. *Endocrinology*. 2011;152:2786-96.
30. Patel PA, Cubbon R., Sapsford RJ, Gillot RG, Grant PJ, Witte KK, Kearney MT, Hall AS. An evaluation of 20 year survival in patients with diabetes mellitus and acute myocardial infarction. *Int J Cardiol*. 2016;203:141-144.
31. Cubbon RM, Adams B, Rajwani , Mercer BN, Patel, PA, Gheradi G, Gale CP, Batin PD, Ajjan, R, Kearney L, Wheatcroft SB, Sapsford RJ, Witte KK, Kearney MT. Diabetes mellitus is associated with adverse prognosis in chronic heart failure of ischaemic and non-ischaemic aetiology. *Diab Vasc Dis Res*. 2013;10:330-336.
32. Marso SP, Hiatt WR. Peripheral Arterial Disease in Patients with Diabetes. *J Am Coll. Cardiol* 2006;47:921-929.
33. Dormandy JA, Charbonnel B, Eckland DJ, et al. PROactive Investigators. Secondary prevention of macrovascular events in patients with type 2 diabetes in the PROactive Study (PROspective pioglitAzone Clinical Trial In macroVascular Events): a randomised controlled trial. *Lancet*. 2005;366:1279-1289.
34. Kubota T, Kubota N, Kumagai H et. al. Impaired insulin signaling in endothelial cells reduces insulin-induced glucose uptake by skeletal muscle. *Cell Metab*. 2011; 13:294-307.
35. Taniguchi CM, Emanuelli B, Kahn CR. Critical nodes in signalling pathways: insights into insulin action. *Nat Rev Mol Cell Biol*. 2006; 7:85-96.
36. Fernandez-Hernando C, Ackah E, Yu J, Suarez Y, Murata T, Iwakiri Y, Prendergast J, Miao RQ, Birnbaum MJ, Sessa WC. Loss of Akt1 leads to severe atherosclerosis and occlusive coronary artery disease. *Cell Metabolism*. 2007;6:446-457.
37. Mukai Y, Rikitake Y, Shiojima I, Wolfrum S, Satoh M, Takeshita K, Hiroi Y, Salomone S, Kim HH, Benjamin LE, Walsh K, Liao JK. Decreased vascular lesion formation in mice with inducible endothelial-specific expression of protein kinase Akt. *J Clin Invest*. 2006;116:334-343.
38. Baumer AT, Ten Freyhaus H, Sauer H, Wartenberg M, Kappert K, Schnabel P, Konkol C, Hescheler J, Vantler M, and Rosenkranz S. Phosphatidylinositol 3-kinase-dependent membrane recruitment of Rac-1 and p47phox is critical for alpha platelet-derived growth factor receptor induced production of reactive oxygen species. *J Biol Chem*. 2008;283:7864-7876.
39. Xia M, Li G, Ma J, Ling W. Phosphoinositide 3-kinase mediates CD40 ligand-induced oxidative stress and endothelial dysfunction via rac1 and NADPH oxidase. *J. Thromb. Haemostasis* . 2009;8:397-406.
40. Brown DI, and Griendling, KK. Nox proteins in signal transduction. *Free Radic Biol Med*. 2009;47:1239-1253.

41. Drummond GR, Selemidis S, Griendling KK, and Sobey CG. Combating oxidative stress in vascular disease: NADPH oxidases as therapeutic targets. *Nat Rev Drug Targets*. 2011;10:453-471.
42. Avraham H, Park SY, Schinkmann K, Avraham S. RAFTK/PYK2-mediated cellular signalling. *Cell Signal*. 2000;12:123-33.
43. Ishikawa M, Pruneda LM, Adams-Hue B, Raskin P. Obesity-independent hyperinsulinemia in nondiabetic first-degree relatives of individuals with type 2 diabetes. *Diabetes*. 1998;47:788-792.
44. Hu G, Qiao Q, Tuomiheto J, Eliasson M, Feskens EJ, Pyorala K, DECODE Insulin Study Group. Plasma insulin and cardiovascular mortality in non-diabetic European men and women: a meta-analysis of data from eleven prospective studies. *Diabetologia*. 2004;47:1245-1256.
45. Noronha BT, Li JM, Wheatcroft SB, Shah AM, Kearney MT. Inducible nitric oxide synthase has divergent effects on vascular and metabolic function in obesity. *Diabetes*. 2005;54:1082-1089.

Figures and legends

Figure 1. Characterisation of mice with endothelial cell-specific over-expression of the human insulin receptor (hIRECO). **A)** Growth (left) and organ weight (right) of hIRECO (n = 11) is no different to wild type (WT, n = 12) littermates. **B)** mRNA expression of human insulin receptor in heart, lungs and spleen from hIRECO and wild type littermate controls (n = 7-8 per group). **C)** mRNA expression of endogenous insulin receptor in organs from hIRECO and wild type littermates (n = 4). **D)** mRNA expression of human insulin receptor (hIR) in endothelial cells (PEC) and non-endothelial cells from hIRECO compared to wild type littermates (n = 4). **E)** mRNA *Ve-Cadherin* expression in endothelial cells from hIRECO with no expression in non-endothelial cells (n = 4). **F)** No change in mRNA expression of native insulin receptor expression in endothelial cells from hIRECO (n = 4). **G)** Western blot (left) showing greater insulin receptor protein expression (right) in endothelial cells from hIRECO (n = 6) compared to wild type littermates (n = 4). Data normalized to WT animals carried out in pairs. (Data presented as mean \pm SEM. * denotes $p < 0.05$; WT vs. hIRECO or hIRECO PEC).

Figure 2. Enhanced endothelial cell insulin sensitivity in mice with endothelium specific over-expression of the human insulin receptor (hIRECO). Representative western blots shows basal levels of tyrosine-phosphorylated insulin receptor (IR-Y) with equal loading (60 microgram), basal eNOS and Akt phosphorylation and dose-response to varying doses of insulin (50 to 150nmol/L; 15 minutes). **A)** Basal (left) and insulin-stimulated (right) tyrosine phosphorylation of insulin receptor were substantially higher in endothelial cells from hIRECO compared to wild type (WT) littermates (n = 4 in each group). **B)** Basal serine phosphorylation of eNOS (left) and the downstream insulin target, protein kinase B/Akt (Akt) (right) in endothelial cells from hIRECO (n = 7 in both groups) was enhanced in endothelial cells from hIRECO compared to wild type littermates. Both groups of mice were sacrificed and lungs were isolated at the same time and therefore, WT was set as one hundred percent as comparison to hIRECO. **C)** Dose response to insulin in endothelial cells demonstrating increased sensitivity to insulin-mediated serine phosphorylation of Akt in endothelial cells from hIRECO (n = 10) compared to wild type littermates (n = 7) (Data presented as mean \pm SEM. * denotes $P < 0.05$ vs. WT control, † denotes $p < 0.05$ vs. hIRECO control).

Figure 3. Metabolic function and systolic blood pressure in mice with endothelial cell specific over-expression of the human insulin receptor (hIRECO). **A)** No difference in fasting glucose between hIRECO (n = 7) and wild type littermates (WT, n = 9). **B)** No difference in fasting insulin between hIRECO and wild type littermates. **C)** No difference in systolic blood pressure between hIRECO (n = 6) and wild type littermates (n = 7). **D)** No difference in glucose tolerance tests between hIRECO (n = 7) and wild type littermates (n = 9). **E)** No difference in insulin tolerance tests between hIRECO (n = 7) and wild type littermates (n = 8). **F)** No difference in triglycerides between hIRECO (n = 8) and wild type littermates (n = 6). **G)** No difference in free fatty acids between hIRECO (n = 7) and wild type littermates (n = 6). Data presented as mean \pm SEM.

Figure 4. Mice with endothelial cell specific over-expression of the human insulin receptor (hIRECO) have blunted responses to the endothelium NO dependent vasodilator acetylcholine and reduced NO bioavailability in response to isometric tension. **A)** Both groups of mice were harvested, isolated and stimulated or studied at the same time in the same conditions. Acetylcholine-mediated vasorelaxation of aortic rings from hIRECO mice is blunted compared to wild type littermates (WT) (n = 6). **B)** No significant differences were observed in phenylephrine-mediated constriction of aortic rings from hIRECO compared to wild type littermates. (n = 5 in each group). **C)** No significant differences were observed in sodium nitroprusside responses of aortic rings from hIRECO compared to wild type littermates. (n = 6 in each group). **D)** Reduced constriction to L-NMMA (0.1 mmol/L; 30 minutes) in hIRECO indicative of reduced nitric oxide bioavailability in response to isometric tension compared to wild type littermates (n = 6 in each group). **E)** Effect of insulin (4 mU/ml; 2 hours) on PE-mediated vasoconstriction is blunted in hIRECO compared to wild type littermates (n = 6 in each group). **F)** Direct insulin-mediated vasorelaxation is blunted in hIRECO compared to WT (left) (n = 7 in each group). L-NMMA significantly blunted insulin-mediated vasodilatation (right) (n = 7 in each group). **G)** Insulin-stimulated eNOS activity in endothelial cells was significantly blunted and was lower in endothelial cells from hIRECO (n = 7) compared to WT (n = 4). Insulin-stimulated eNOS activity of each type of mouse was compared against its own unstimulated control, set as one hundred percent. (Insulin 150 nmol/L; 45 minutes). **H)** Representative western blots shows shear stress-induced Akt and eNOS phosphorylation. Shear stress-mediated serine-473 phosphorylation of Akt (12 dyne/cm²; 10 minutes) was not different between both groups of mice (n = 8-9). **I)** In hIRECO endothelial cells shear stress-mediated serine-1177 phosphorylation of eNOS was blunted (n = 4) when compared to WT (n = 6). (Data presented as mean ± SEM. In western blot, TG denotes hIRECO. * P<0.05 vs. unstimulated or uninhibited controls).

Figure 5. Role of oxidative stress in reduced NO bioavailability in mice with endothelial cell specific over-expression of the human insulin receptor (hIRECO). **A)** Restoration of acetylcholine-mediated vasorelaxation of aortic rings from hIRECO (n = 7 in each group) after exposure of rings to the superoxide dismutase mimetic, MnTmPyP (10 micromol/L, 30 minutes). **B)** Acetylcholine-mediated vasorelaxation of aortic rings from hIRECO (n = 8 in each group) after exposure to the Nox2 NADPH oxidase inhibitor, gp91ds-tat (gp;10 micromol/L; 30 minutes) was restored to wild type littermates' (WT) level. **C)** NADPH-dependent superoxide generation in endothelial cells from hIRECO mice is increased in lucigenin-enhanced chemiluminescence assay (n = 10 in each group). **D)** Increased expression of Nox2 NADPH oxidase in endothelial cells from hIRECO (n = 7). **E) left** Endothelial cells from hIRECO treated with Nox2 inhibitor, gp91ds-tat (gptat; 10 micromol/L; 60 minutes) have reduced superoxide production by chemiluminescence analysis of superoxide generation **E) centre** gp91ds-tat inhibitable superoxide production was significantly greater in hIRECO than WT by DHE HPLC-based assay, presented as percentage difference from uninhibited control (n = 10 in each group) **E) right** Amplex Red quantification of hydrogen peroxide showed increased levels of hydrogen peroxide in hIRECO cells compared to WT (n = 5 in each group). **F)** Chronic treatment of hIRECO with the Nox2 inhibitor gp91ds-tat or scrambled (Scr) control for 28 days had no effect on body mass (n = 8 in each group). **G)** Chronic treatment of hIRECO with the Nox2 inhibitor, gp91ds-tat or scrambled (Scr) control for 28 days had no effect on glucose (left) or insulin tolerance (right) (n = 6 in each group). **H)** Chronic treatment of hIRECO with the Nox2 inhibitor gp91dstat (10 micromol/L) for 28 days increased maximal relaxation of aortic rings to acetylcholine compared to scrambled (Scr) control (n = 6 in each group). (Data presented as mean ± SEM. * denotes P<0.05 WT vs. hIRECO, † denotes P<0.05 hIRECO vs. hIRECO+gp91ds-tat).

Figure 6. Insulin mediated generation of superoxide is enhanced in endothelial cells from mice with endothelial cell specific over-expression of the human insulin receptor (hIRECO) and is PI3K- and Akt-dependent. Increased tyrosine phosphorylated eNOS and increased expression of proline rich tyrosine kinase (PYK2) in hIRECO mice. **A**) Role of PI3-kinase in excess superoxide production in endothelial cells from hIRECO was confirmed by the PI3-kinase specific inhibitor Wortmannin (WM, 50 nanomol/L; 30 minutes) and a complementary the PI3-kinase specific inhibitor **B**) LY294002 (LY, 5 micromol/L; 30 minutes), both of which reduced superoxide production in hIRECO endothelial cells to a greater extent than wild type (n = 5). **C**) The Akt inhibitor MK-2206 (MK, 10 micromol/L; 3 hours) reduced superoxide generation from hIRECO endothelial cells (n = 4-5). **D**) Insulin-stimulated (Ins, 150 nmol/L; 3 hours) superoxide release was reduced in endothelial cells from hIRECO by the inhibitor of Nox2 NADPH oxidase gp91ds-tat (gptat, 10 micromol/L; 60 minutes) and Akt inhibitor, MK-2206 (MK; 10micromol/L; 60 minutes) (n = 10). Representative blots showing eNOS-pY657, eNOS-pS1177 (eNOS-p), PYK2 expressions in various experimental conditions, as stated on the far left panel. **E**) (left) Increased tyrosine 657-phosphorylated eNOS in hIRECO endothelial cells compared to wild type littermates (n = 5), (right) Inhibition of NOX2 by gp91ds-tat led to reduced tyrosine-657 phosphorylation of eNOS. **F**) Proline-rich tyrosine kinase 2 (PYK2) expression is increased in hIRECO endothelial cells (n = 4). **G**) Gene silencing of PYK2 in hIRECO endothelial cells using siRNA resulted in approximately 50% knockdown compared to scrambled (Scr siRNA) siRNA control (n = 5). **H**) Insulin-stimulated eNOS activity was reversed in hIRECO endothelial cells upon PYK2 siRNA (siPYK2) knockdown (n = 5). **I**) Shear stress-induced (Shear) eNOS phosphorylation was restored in hIRECO endothelial cells following PYK2 siRNA knockdown (n = 6). (Data presented as mean \pm SEM. * denotes $P < 0.05$ WT vs hIRECO or Control vs WM, LY, MK, Insulin, gptat, PYK2 siRNA, † denotes $P < 0.05$ (hIRECO+Insulin/shear stress) vs. (hIRECO + PYK2 siRNA+Insulin/shear stress), hIRECO Ins vs. (hIRECO MK+Ins), †† denotes $P < 0.05$ hIRECO+Ins vs. hIRECO gptat+Ins).

Figure 7. Crosstalk between Nox2 and PYK2 in endothelial cells from mice with endothelial cell specific over-expression of the human insulin receptor (hIRECO). Left panel shows representative blots for PYK2 phosphorylation (PYK2-p) PYK2, and beta-actin loading control; eNOS and Nox2 in various experimental conditions studied. **A**) Inhibiting basal Nox2 activity with gp91-dstat (gptat) and inhibition of Akt by MK-2206 (MK, 10 mol/L; 8 hours) in endothelial cells from hIRECO reduced PYK2 expression (n = 5). **B**) Reducing basal Nox2 expression with siRNA in hIRECO endothelial cells also reduced PYK2 expression. **C**) Knock-down of PYK2 in hIRECO (HIR) endothelial cells using siRNA reduced Nox2 expression (n=4-5). **D**) Knockdown of PYK2 (PYK2) and not NOX2 (siNOX2) using siRNA in endothelial cells of hIRECO significantly enhanced insulin-stimulated (Ins, 150 nanomol/L; 15 minutes) serine-phosphorylation of eNOS (n=6). Percentage phosphorylation was assessed by normalizing against unstimulated control of each mouse. (Data presented as mean \pm SEM. * denotes $P < 0.05$ wild type (WT) vs hIRECO, † denotes $P < 0.05$ hIRECO vs. hIRECO siRNA PYK2, hIRECO vs. hIRECO siRNA-NOX2, hIRECO vs. hIR siRNA PYK2, hIRECO Ins vs. hIRECO PYK2+Ins).

Figure 8. Endothelial-specific over-expression of human insulin receptor mice (hIRECO) have increased atherosclerosis when crossed onto an ApoE-deficient background (ApoE^{-/-}/hIRECO). **A**) No difference in body weight after 12 weeks western diet in ApoE^{-/-}/hIRECO compared to ApoE^{-/-} littermates. **B**) Systolic blood pressure after 12 weeks western diet in ApoE^{-/-}/hIRECO compared to ApoE^{-/-} littermates **C**) No difference in fasting cholesterol in ApoE^{-/-}/hIRECO compared to ApoE^{-/-} littermates. **D**) No difference in fasting triglycerides in ApoE^{-/-}/hIRECO compared to ApoE^{-/-} littermates. **E**) No difference in fasting blood glucose levels or **F**) No difference in glucose tolerance or **G**) insulin tolerance testing after 12 weeks western diet in ApoE^{-/-}/hIRECO compared to ApoE^{-/-} littermates **H**) Increased

plaque development in the thoracic aorta in ApoE^{-/-}/hIRECO mice compared to ApoE^{-/-} littermates. **I)** Increased plaque development at the level of the aortic sinus in ApoE^{-/-}/hIRECO mice compared to ApoE^{-/-} littermates **J)** Proposed mechanism of downstream effects of increased insulin sensitivity in the endothelium. (Data presented as mean ± SEM. n = 15 mice per group, * denotes P<0.05, ApoE^{-/-} vs. ApoE^{-/-}/hIRECO; + denotes stimulatory effect,- denotes inhibitory effect).

Novelty and Significance

What is known?

- Insulin binds to its tyrosine kinase receptor to activate downstream signalling molecules including Akt/PKB leading to activation of endothelial nitric oxide synthase (eNOS) which stimulates production of the antiatherosclerotic signalling radical nitric oxide.
- Resistance to the action of insulin in the endothelium a well-established feature of type 2 diabetes leads to a proatherosclerotic imbalance between nitric oxide and superoxide.
- Mice with endothelium specific insulin resistance develop accelerated atherosclerosis.

What new information does this article contribute?

- Over expressing insulin receptors in the endothelium increases insulin mediated activation of Akt.
- Over expressing insulin receptors in the endothelium leads to PYK2 mediated inhibition of eNOS and increased generation of superoxide, the enzymatic source of which was the Nox 2 isoform of NADPH oxidase.
- Over expressing insulin receptors in the endothelium accelerated the development of atherosclerosis in hyperlipidaemic apolipoprotein E-deficient mice.

Type 2 diabetes is associated with whole body and endothelial cell insulin resistance. While the proatherosclerotic effect of endothelial cell insulin resistance is well established, the effect of enhancing insulin sensitivity in the endothelium remains unclear. To examine the effect of selective enhancement of insulin sensitivity in the endothelium we generated transgenic mice with endothelium specific over expression of insulin receptors.

In mice with endothelium specific over expression of insulin receptors both insulin and acetylcholine mediated vasorelaxation of aortic rings was blunted. The impaired relaxation in response to acetylcholine was restored by the Nox2 NADPH oxidase (Nox2) specific inhibitor gp91^{dstat}. Further probing the mechanisms underlying these findings we showed that insulin mediated Akt phosphorylation in endothelial cells was enhanced which increased Nox2 generated superoxide. In addition to this proatherosclerotic perturbation, we also demonstrated an Akt and Nox2 dependent increase in expression of the non-receptor tyrosine kinase PYK2 which fed back to increase Nox2 expression and downstream led to inhibitory tyrosine phosphorylation of eNOS.

This work reveals a previously unrecognised insulin activated proatherosclerotic signalling circuit involving Nox2, Akt, PYK2 and eNOS. Increasing insulin sensitivity in the endothelium activates and amplifies this loop to drive the development of atherosclerosis.

SUPPLEMENTAL MATERIALS

Selective enhancement of insulin sensitivity in the endothelium *in vivo* reveals a novel proatherosclerotic signalling loop.

First Author's Surname: Viswambharan

Short Title: Insulin sensitivity and NO availability

Hema Viswambharan PhD, Nadira Yuldasheva PhD, Anshuman Sengupta MBChB PhD, Helen Imrie PhD, ²Matthew Gage PhD, Natalie Haywood PhD, Andrew MN Walker MBChB BSc, Anna Skromna MSc, Natallia Makova MSc, Stacey Galloway BSc, Pooja Shah BSc, Piruthivi Sukumar PhD, Karen E Porter PhD, Peter J Grant MD, FMedSci, ¹Ajay M Shah MD, FMedSci, ¹Celio XC Santos PhD, Jing Li PhD, David J Beech PhD, FMedSci, Stephen B Wheatcroft MBBS FRCP, Richard M Cubbon MBChB, PhD, Mark T Kearney DM, FRCP.

Leeds Institute of Cardiovascular and Metabolic Medicine, University of Leeds. ¹British Heart Foundation Centre of Research Excellence, King's College London. ²Metabolism & Experimental Therapeutics, Division of Medicine, University College London.

SUPPLEMENTAL MATERIALS

Detailed and Extended Methods

Mice over expressing the human insulin receptor specific to the endothelium.

To overcome the limitations seen in standard transgenics we used the Hypoxanthine Phosphoribosyl transferase (*Hprt*) targeting system¹ applying 'Quick Knock-inTM' (GenOway) technology to generate genetically modified embryonic stem (ES) cells. This approach uses homologous recombination to target a single copy of a transgene (in this case the human IR) driven by a promoter (in this case the *Tie2* promoter) into the *Hprt* locus on the X chromosome (Supplemental Figure IA).

As previously described² the model was developed with E15Tg2a (E14) cells derived from the strain 129P2/OlaHsd (12901a). In E14 cells, 35kb of the *Hprt* gene encompassing the 5' UTR up to intron 2 is deleted. The *Hprt* gene encodes a constitutively expressed housekeeping enzyme involved in purine synthesis from the degradation products of nucleotide bases (salvage pathway). Cells normally synthesise purines by the salvage and *de-novo* pathways. In *Hprt* deleted cell lines, only the *de-novo* pathway is functional enabling the cells to grow in classical medium. However, in the presence of the aminopterin drug the *de-novo* pathway is blocked. As a result *Hprt* deleted cells die in media called HAT (containing hypoxanthine, aminopterin and thymidine substrates). The targeted insertion of a transgenic cassette in E14 ES cells with a functional *Hprt* gene rescues these cells, which can then be selected using HAT media to identify ES cells showing the correct targeting event. Thus ES cells with the correct insertion can be selected by virtue of their expression of *Hprt* and the resultant ability to grow in HAT medium. Numerous studies have shown that the functional properties of the *Hprt* locus protect transgenic constructs inserted in this region against gene silencing and positional or methylation effects. Furthermore, tissue-specific promoters including *Tie2* inserted³ into the *Hprt* locus maintains their expression properties. This sequence has been shown confer uniform and high level of expression of Lac Z reporter gene in endothelial cells *in vivo*.

Vector construction. Endothelial cell-specific transgene expression was achieved using the mouse *Tie2* promoter and intronic enhancer as previously described. In order to reduce the size of

transgene the minimal-enhancer sequence (core-enhancer) was inserted into the final construct. This sequence has been shown confer uniform and high level of expression of Lac Z reporter gene in endothelial cells in vivo. The targeting vector was obtained by inserting human IR cDNA (a kind gift from Dr M Quon NIH Bethesda USA) into the pHNS plasmid comprising the murine Tie2 promoter, LacZ cDNA and SV40 polyA signal and a 10-kb intronic enhancer from the murine Tie2. The targeting vector was obtained by inserting human IR cDNA (a kind gift from Dr M Quon NIH Bethesda USA) into the pHNS plasmid comprising the murine Tie2 promoter, LacZ cDNA and SV40 polyA signal and a 10-kb intronic enhancer² from the murine Tie2. The final transgenic vector consisting of Tie2 promoter, human IR, polyadenylation site and core-enhancer was then inserted into the Hprt targeting vector by a gateway reaction between the transgenic vector and the Hprt targeting vector. The final targeting vector had the following features; 1) Isogenic with E14 ES cells favouring homologous recombination, 2) Symmetrical homology arms (5' short arms-SA: 3.8kb, 3' long arm -LA: 3.7kb), 3) Transgenic cassette expressing the human IR cDNA under control of the short form of the Tie2 promoter, 4) Wild type Hprt sequences to reconstitute the Hprt gene in the E14 ES cells. In ES cells, this process was highly successful with 3 clones selected for blastocyst injection. The 5' and 3' targeting events were unambiguously confirmed by Southern blot analysis. These 3 ES clones were expanded and genetically manipulated agouti ES cells were then injected into C57BL/6J derived blastocysts that were then implanted into the uteri of recipient females.

Breeding of Chimeras and generation of F1 mice heterozygous for the human insulin receptor. Highly chimeric males (displaying 100% chimerism) generated by blastocyst injection of ES clones were mated with 2 wild type C57BL/6J female mice, to examine whether the targeted ES cells contributed to the germ layer. To assess whether ES cells have contributed to the germ layer of chimeras, mouse coat colour markers are used. The ES cells used to develop the model were originally derived from a 129 strain of mice which have an agouti coat colour. This marker is dominant over the black coat of C57BL/6 mice. Therefore, mating of the chimeras with C57BL/6J mice yields agouti coloured pups when the ES cells have contributed to the germ layer. Agouti F1 females were genotyped by Southern blot (Supplemental Figure IB). Southern blot validated the correct heterozygous status of tested F1 females, by detecting the 15.2 kb sized AvrII fragment of the C57BL/6 Hprt wild type allele and the 9.8kb sized AvrII fragment of the reconstituted Hprt allele (females #2, #4, #6, #7, (Supplemental Figure IB). Genotyping protocol validated the multiple copies of transgene (Supplemental Figure IC). Two of the F1 females were backcrossed for at least 10 generations into a C57BL/6J background and genotyped (Supplemental Figure ID) before commencing experiments.

All experiments were carried out comparing with wild type littermate controls. Genotyping PCR primer sequence (5' to 3'): Primer 1, ACGTCAGTAGTCATAGGAAGTGC GGTCG and Primer 2, TGCCTTGATTCACCATGCTGAGG.

High performance liquid chromatographic measurement of conversion of dihydroethidium to oxyethidium. Aortic segments were incubated with scrambled peptide or the *Nox2* specific inhibitor, gp91-dstat for 30 minutes in KREBS buffer and then washed twice with PBS before incubating in PBS/DHE at a final concentration of 100 µmol/L for 30 min. Cells were washed thrice with cold PBS, harvested in cold methanol/HCl (0.5 ml/well), vortexed vigorously, centrifuged (12,000 *g* for 10 min at 4°C), and supernatants recovered for analysis. Pellets were stored at -20°C in the dark until analysis. Samples were injected (30µL), into an HPLC system (Shimadzu), equipped with a photodiode array (SPD-M10AVP) and fluorescence (RF-10AXL) detectors. Chromatographic separation was carried out in a C18-Kromosil column (4.6 x 250 mm, 5 µm particle size) and DHE monitored by ultraviolet absorption at 245 nm and EOH and ethidium by fluorescence detection (excitation 510 nm and emission 595 nm). Quantification is performed by comparison of peak signal between the samples and standard solutions under identical chromatographic conditions²⁵. DHE-derived products are expressed as ratios of ethidium generated per DHE consumed (ethidium/DHE) and normalized against total weight of tissue. Data expressed as gp91ds-tat-inhibitable component of superoxide.

Amplex red assay for hydrogen peroxide in aorta. Freshly harvested aortas were collected into a modified Krebs-HEPES buffer, containing 20 mM HEPES, 119 mM NaCl, 4.6 mM KCl, 1 mM MgSO₄·7H₂O, 0.15 mM Na₂HPO₄, 0.4 mM KH₂PO₄, 5 mM NaHCO₃, 1.2 mM CaCl₂ and 5.5 mM glucose, pH 7.4. The aortas were cleaned of peripheral adipose tissue and divided in about 2mm aortic rings.² Half of the aortic rings were incubated in 50µL of modified Krebs-HEPES buffer and the remaining aortic rings were incubated in 50µL of modified Krebs-HEPES buffer with 1250 U/mL catalase (free from tymol) for 1h at 37°C. Fifty microlitres of freshly-prepared 100 µM Amplex Red reagent with 0.2U/mL HRP was added to the samples and incubated for 1 hour at 37°C, protected from light. The aortic rings were removed from the samples and fluorescence was measured on VarioSkan (Thermo Scientific) plate reader (excitation 530 nm and emission 590 nm). The average readings with catalase were subtracted from average readings without catalase, and the value was used as input into an H₂O₂ standard curve. The H₂O₂ standard curve was prepared in the same plate simultaneously, with the tissues and was used to determine H₂O₂ concentration released in the samples. Weight of blotted dry tissue was used for normalization.

Pulmonary endothelial cell isolation and culture. Lungs were harvested, washed, finely minced and digested in HBSS containing 0.18U/ml collagenase type 2 (Worthington, USA) and for 45 minutes at 37°C⁵. The digested tissue was filtered through a 70µm cell strainer and centrifuged at 1200 rpm for 5 minutes. The cell pellet was washed with PBS/0.2% BSA, centrifuged, resuspended in 100µl of PBS/0.2%FCS and incubated with 1 x 10⁶ CD146-Ab-coated beads at 4°C for 15 minutes^{1,6}. Bead-bound cells were separated from non-bead bound cells using a magnetic MS Column (Miltenyi Biotechnology). Bead-bound (CD146-positive) and non-bead-bound cells were resuspended in 2 ml Endothelial growth medium–MV2 (PromoCell, Heidelberg, Germany) supplemented with hEGF, hydrocortisone, VEGF, hFGF-B, R3-IGF-1, ascorbic acid, gentamicin, amphotericin-B and 5% FCS and plated out. Only the endothelial cell population tested positive for a range of endothelial markers including eNOS, Tie2, ve-cadherin, vWF and CD102 protein measured using immunoblotting.

Characterisation of isolated pulmonary endothelial cells using Dil-Ac-LDL

The endothelial phenotype of PEC was corroborated by demonstrating uptake of acetylated low-density lipoprotein cholesterol (Ac-LDL). Confluent PEC were incubated in standard culture medium containing 10ug/ml Dil-conjugated Ac-LDL (Molecular Probes, ThermoFisher Scientific) for one hour, prior to washing with PBS and fixing with 4% paraformaldehyde in PBS. Imaging was performed using an Olympus CKX-41 microscope using a red fluorescence emission filter. No fluorescence was detected in PEC not exposed to Dil-conjugated Ac-LDL.

Cell lysis, Immunoblotting. Primary endothelial cells were lysed in extraction buffer containing 50mM HEPES, 120mM NaCl, 1mM MgCl₂, 1mM CaCl₂, 10mM NaP₂O₇, 20mM NaF, 1mM EDTA, 10% glycerol, 1% NP40, 2mM sodium orthovanadate, 0.5µg/ml leupeptin, 0.2mM PMSF, and 0.5µg/ml aprotinin. Insulin-stimulated endothelial cells were serum-deprived overnight with 1% FCS-containing endothelial cell media before stimulation and harvesting in lysis buffer for western blot analysis⁶. Cell extracts were sonicated in an ice-bath and centrifuged for 15 minutes at 13000 rpm, before protein measurements were carried out by BCA assay (Pierce Protein Quantification Kit) using the supernatant. Equal amounts of cellular protein were resolved on SDS polyacrylamide gels (Invitrogen) and transferred to polyvinylidene difluoride membranes. Immunoblotting was carried out with indicated primary antibodies, diluted as necessary in 5% BSA-TBST buffer. Blots were incubated with appropriate HRP-conjugated secondary antibodies and developed with enhanced chemiluminescence (Millipore). Sixty micrograms of total cell lysate was used for immunoprecipitation and thirty micrograms for western blotting with indicated antibodies: IR beta (C19) and β-Actin, (Santa Cruz Biotechnology), phospho-tyrosine, (pY4G10, Millipore), Nox2, eNOS, phospho-eNOS (BD Biosciences), PYK2, phospho-PYK2, Akt and phospho-Akt, (Cell Signalling), and phospho-tyrosine 657 (ECM Biosciences) and Protein A-Dynabeads (Invitrogen) for 20 minutes at room temperature. Akt inhibitor, MK-2206 10 micromol/L was from SelleckChem. Immunoblots were scanned on a Syngene Gel Documentation System and bands quantified using Syngene

Genetools Image Analysis software. Where bar charts depict percentage of control or wild type, we carried out all experiments for the two groups of mice (wild type and hIRECO) in pairs using the same conditions; from harvesting organs, isolating cells and stimulation of insulin or various inhibitors/siRNA and therefore, set its own wild type or serum-deprived control wells as hundred percent. When responses to insulin or inhibitors were analysed, the experiments were serum-deprived in 0.5% serum containing medium without supplements overnight before carrying out stimulation and harvesting. Chronic inhibition in cells to analyse protein expression was been performed in full growth medium and inhibitors incubated for 8 hours prior to harvest.

References

1. Imrie H, Viswambharan H, Sukumar P et al. Novel role of the IGF-1 receptor in endothelial function and repair: studies in endothelium-targeted IGF-1 receptor transgenic mice. *Diabetes*. 2012;61:2359-2368.
2. Minami T, Kuivenhoven JA, Evans V, Kodama T, Rosenberg RD, Aird WC. Ets motifs are necessary for endothelial cell-specific expression of a 723-bp Tie-2 promoter/enhancer in Hprt targeted transgenic mice. *Arterioscler Thromb Vasc Biol*. 2003;23:2041-2047.
3. Guillot PV, Liu L, Kuivenhoven JA, Guan J, Rosenberg RD, Aird WC. Targeting of human eNOS promoter to the Hprt locus of mice leads to tissue-restricted transgene expression. *Physiol Genomics*. 2000;2:77-83.
4. Duncan ER, Crossey PA, Walker S, Anilkumar N, Poston L, Douglas G, Ezzat VA, Wheatcroft SB, Shah AM, Kearney MT. Effect of endothelium specific insulin resistance on endothelial function in vivo. *Diabetes*. 2008;57:3307-3314.
5. Abbas A, Imrie H, Viswambharan H, et al. The Insulin-Like Growth Factor-1 Receptor Is a Negative Regulator of Nitric Oxide Bioavailability and Insulin Sensitivity in the Endothelium. *Diabetes*. 2011;60:2169-2178.
6. Wheatcroft SB, Shah AM, Li JM, Duncan E, Noronha BT, Crossey PA, Kearney, MT. Preserved glucoregulation but attenuation of the vascular actions of insulin in mice heterozygous for knockout of the insulin receptor. *Diabetes*. 2004;53:2645-2652.

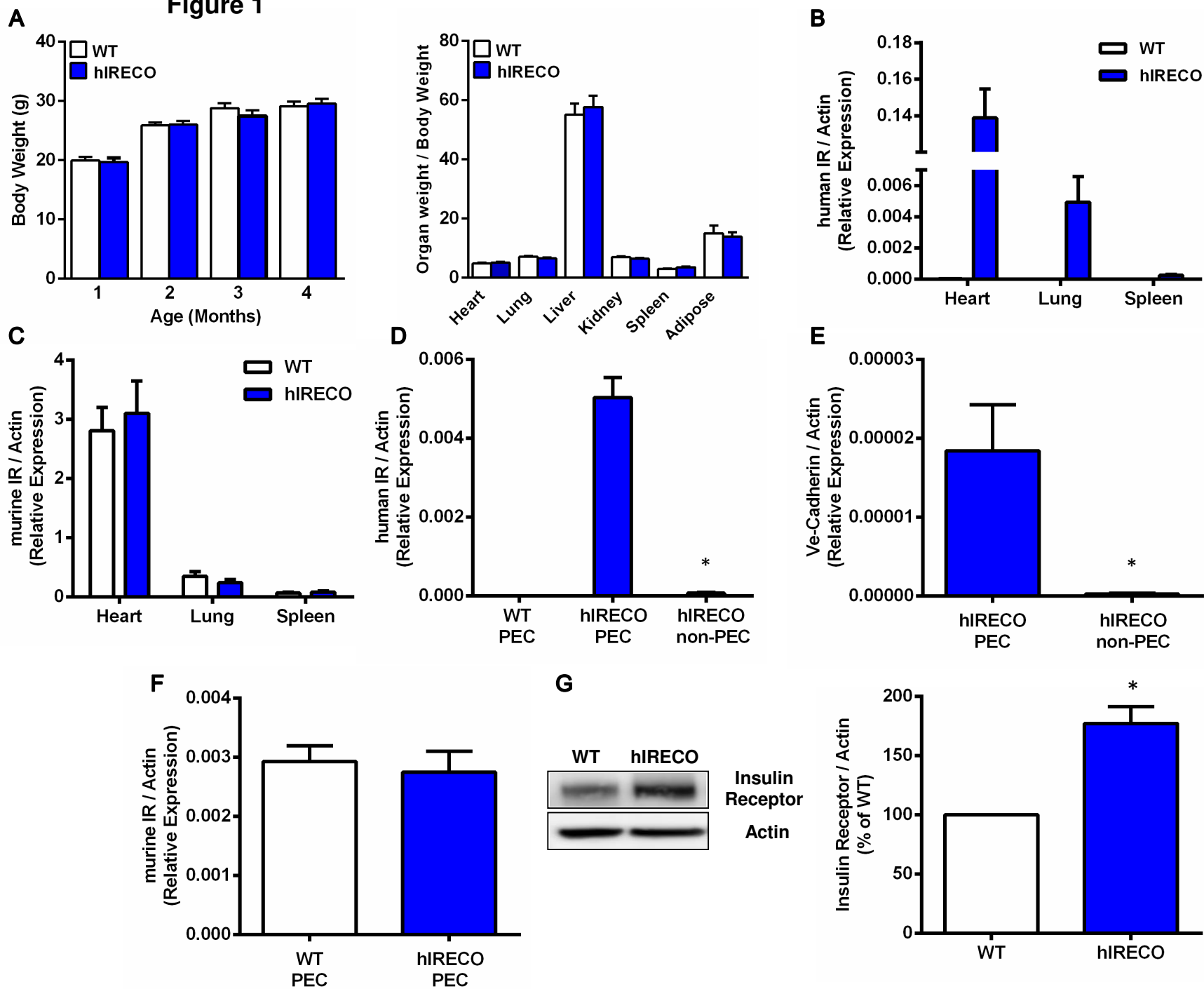
Figure 1

Figure 2

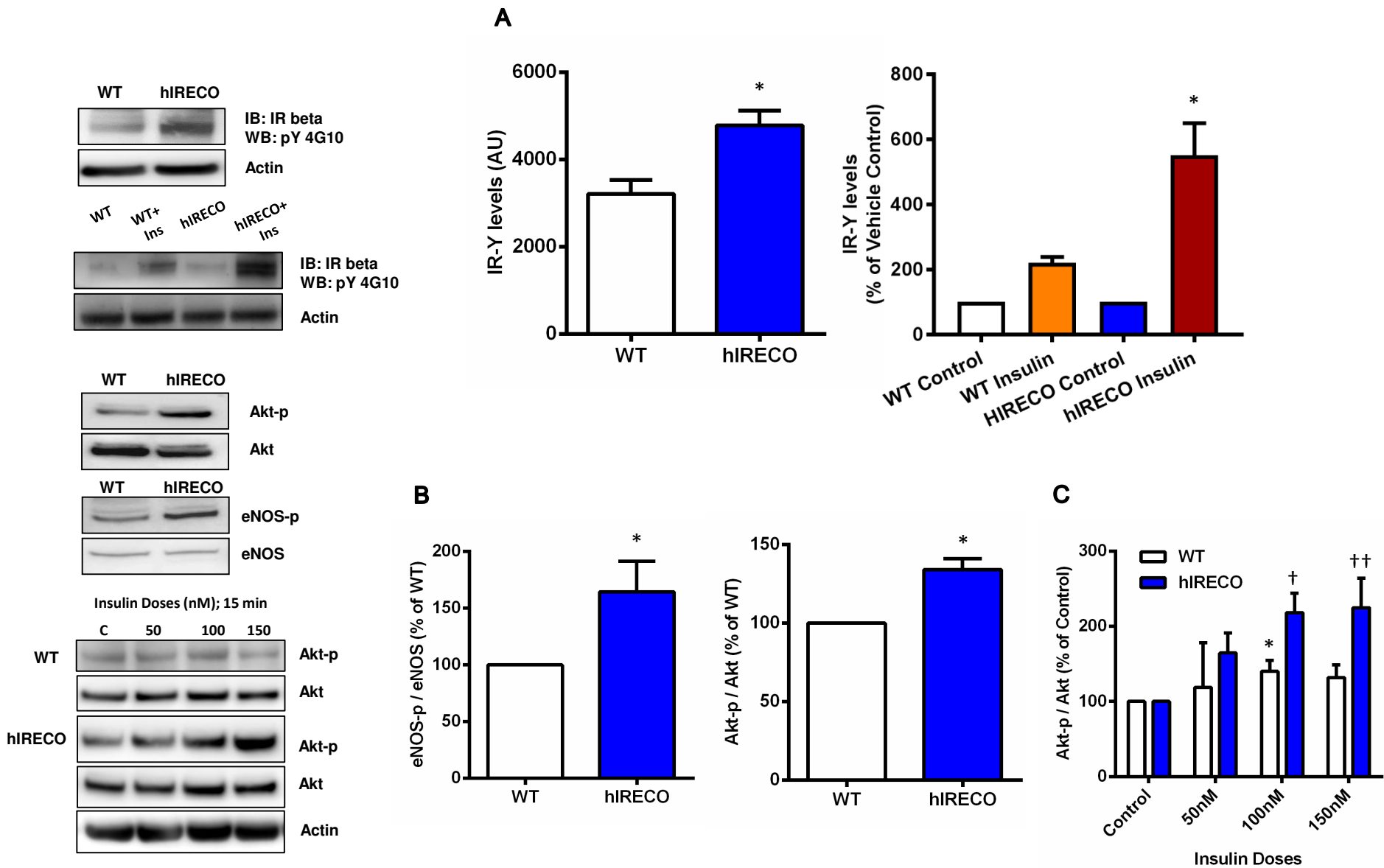


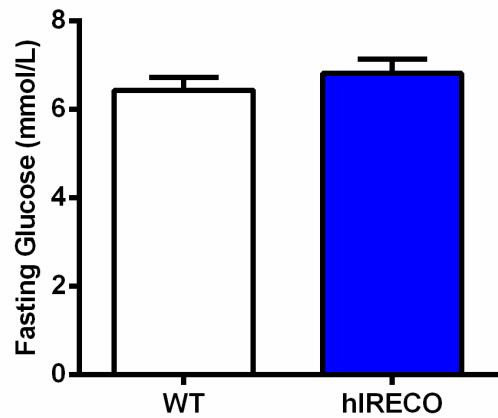
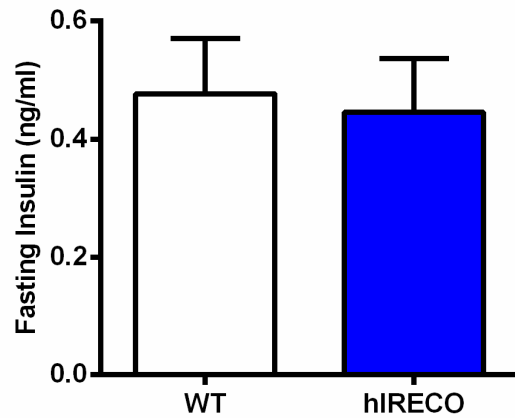
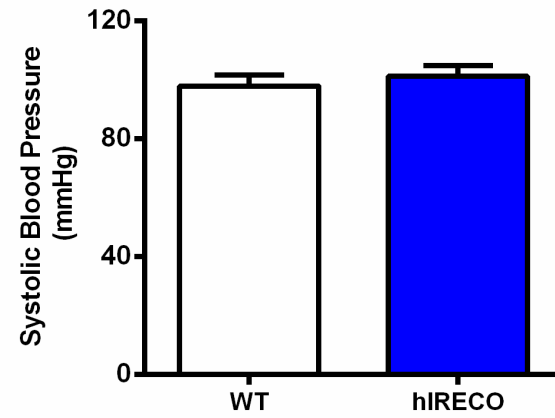
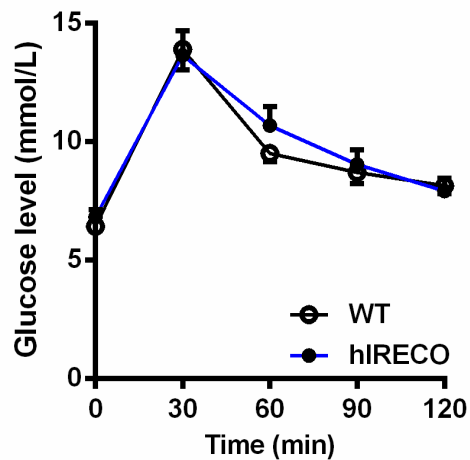
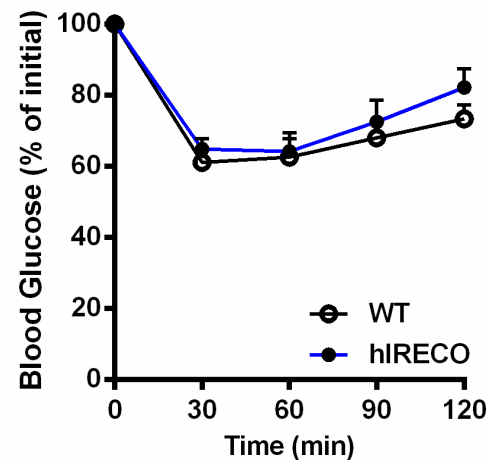
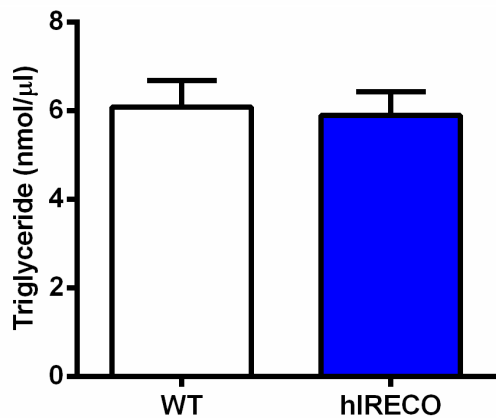
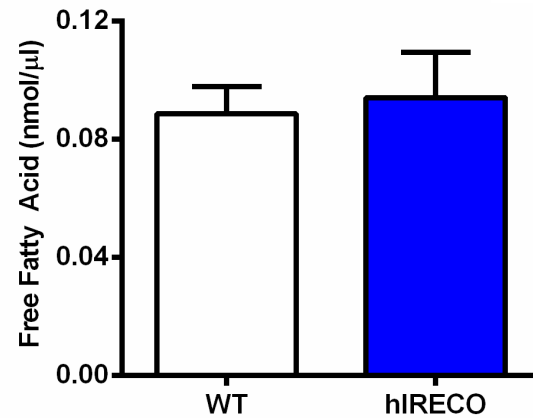
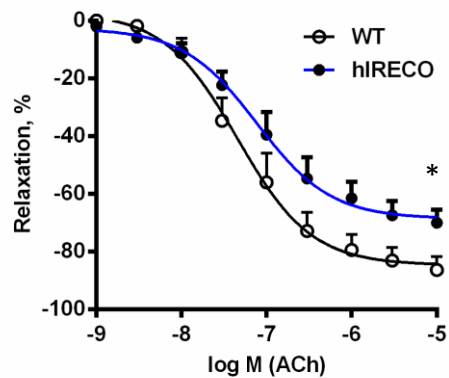
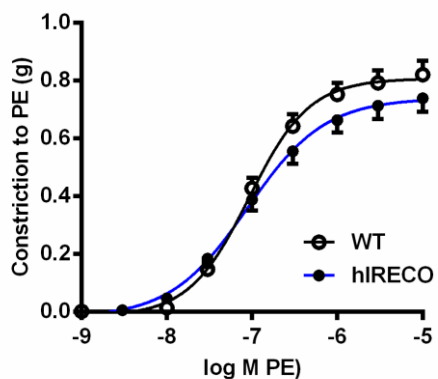
Figure 3**A****B****C****D****E****F****G**

Figure 4

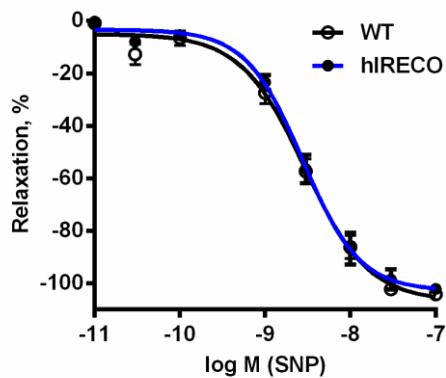
A



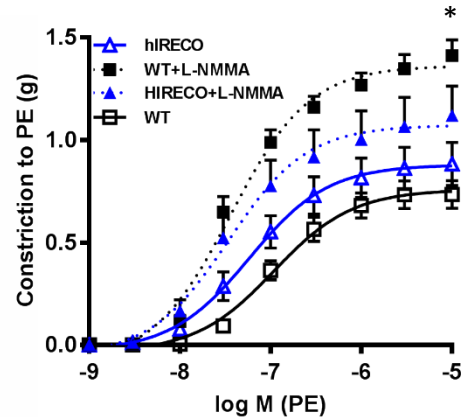
B



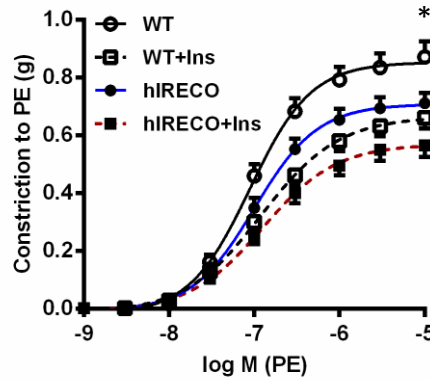
C



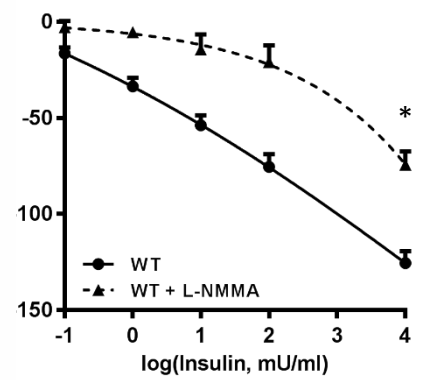
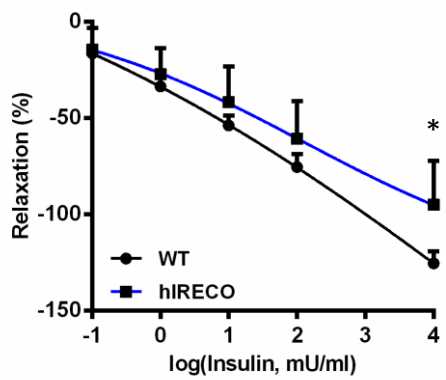
D



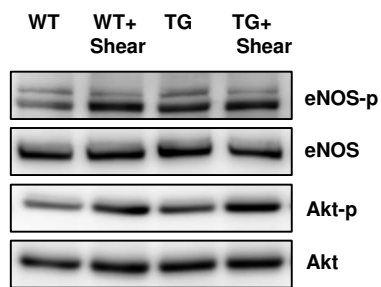
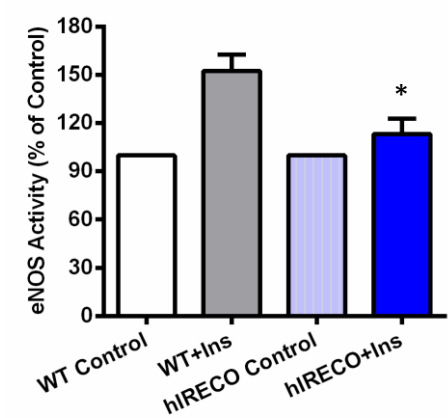
E



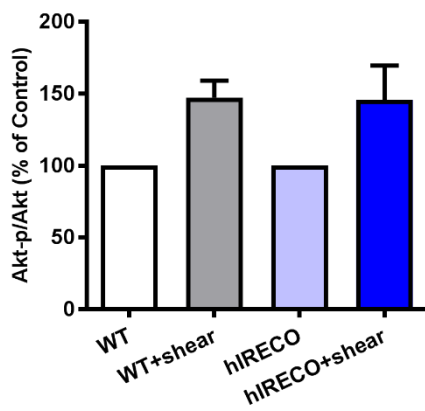
F



G



H



I

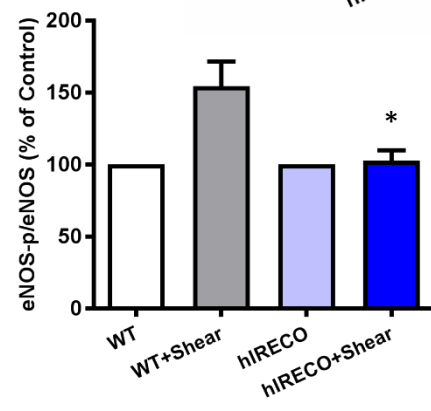


Figure 5

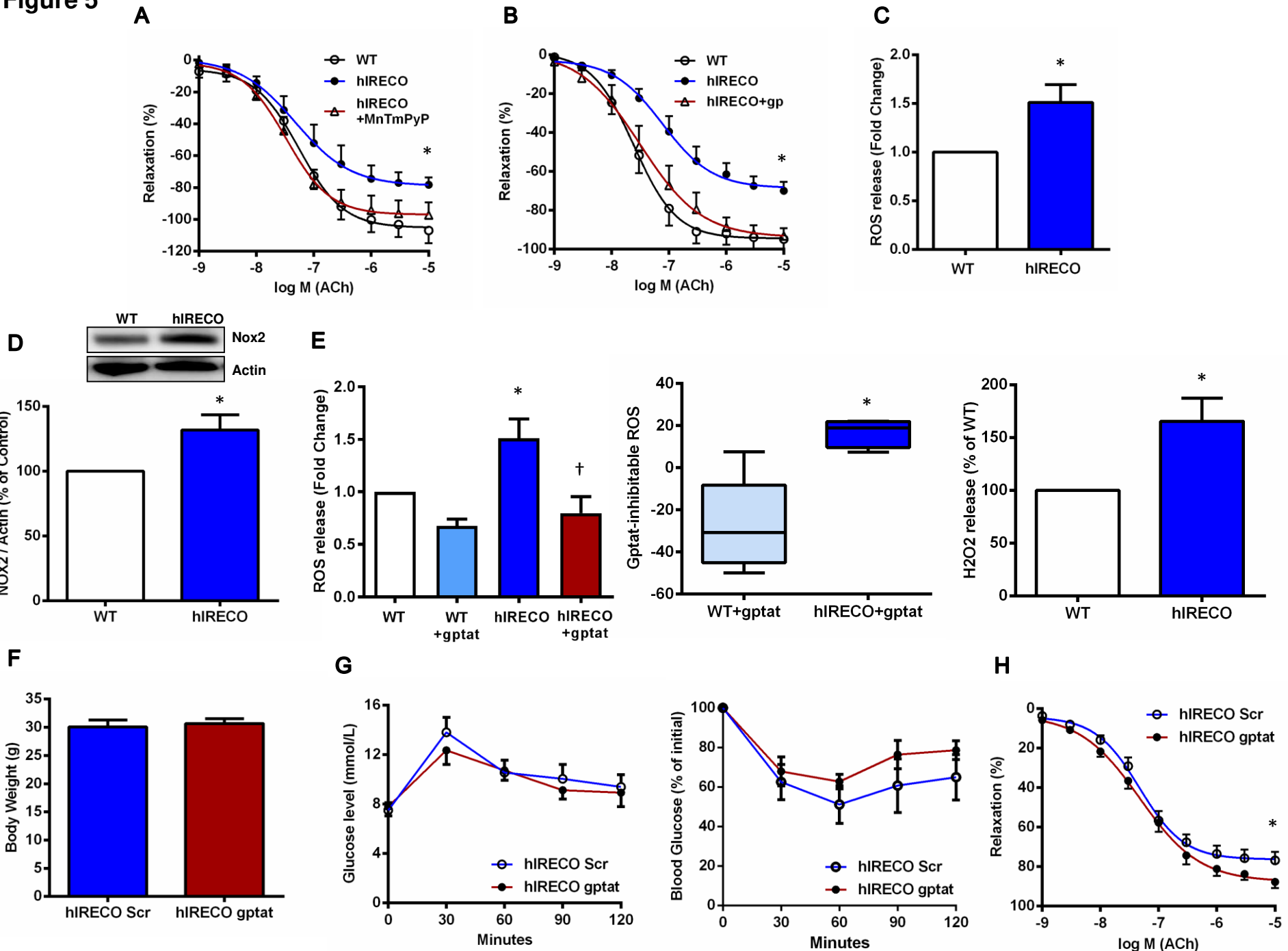
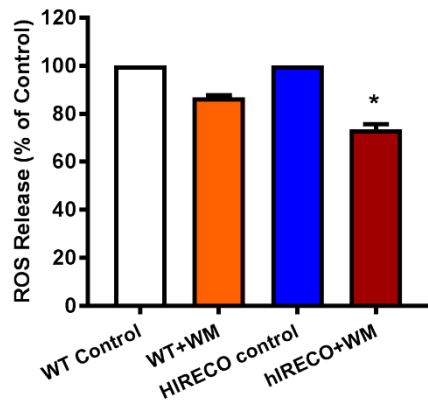
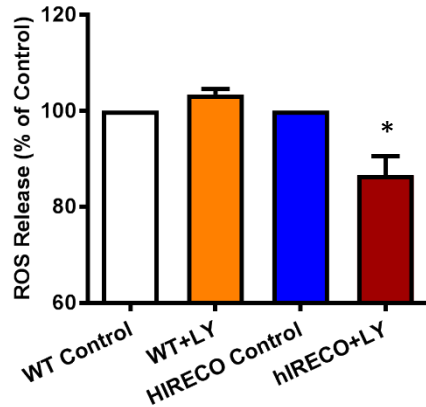


Figure 6

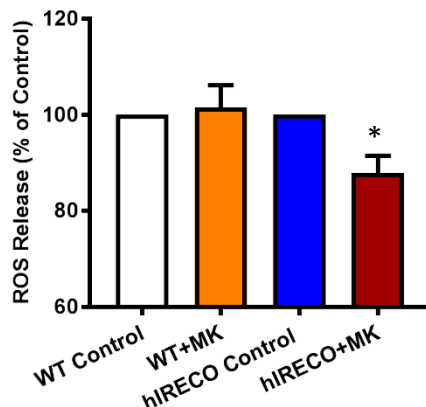
A



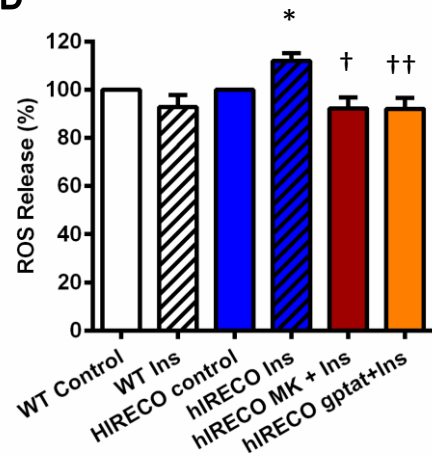
B



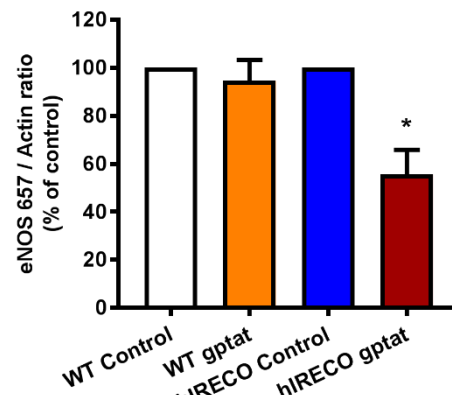
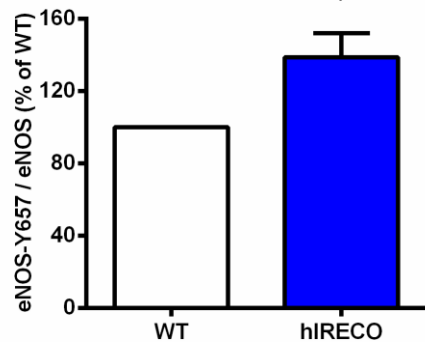
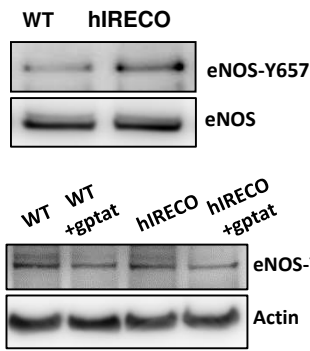
C



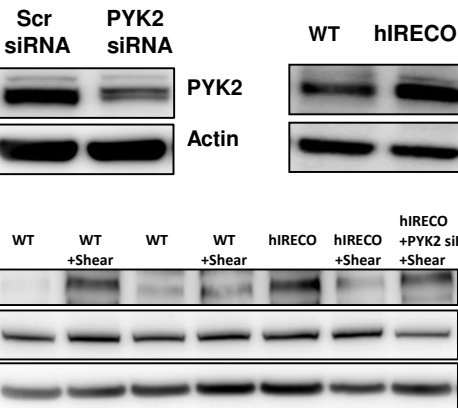
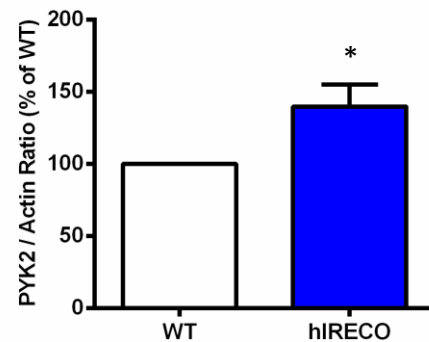
D



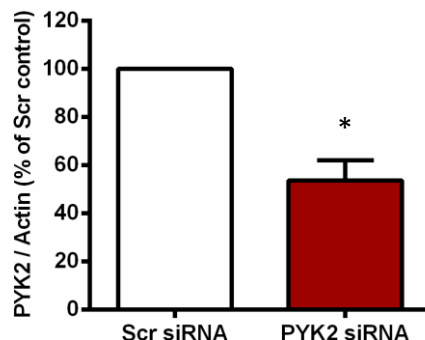
E



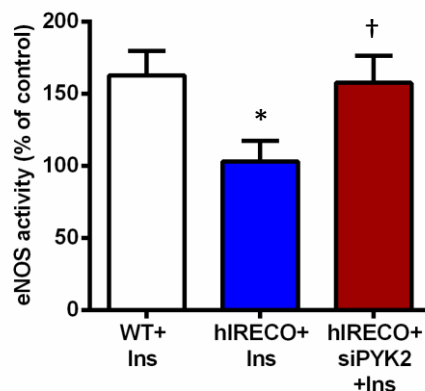
F



G



H



I

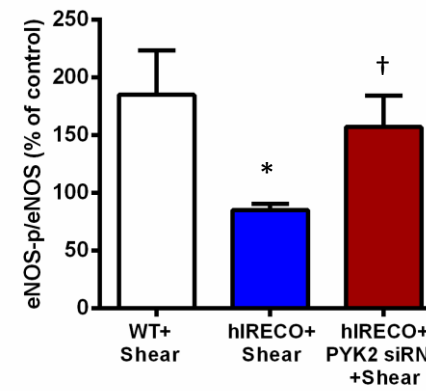


Figure 7

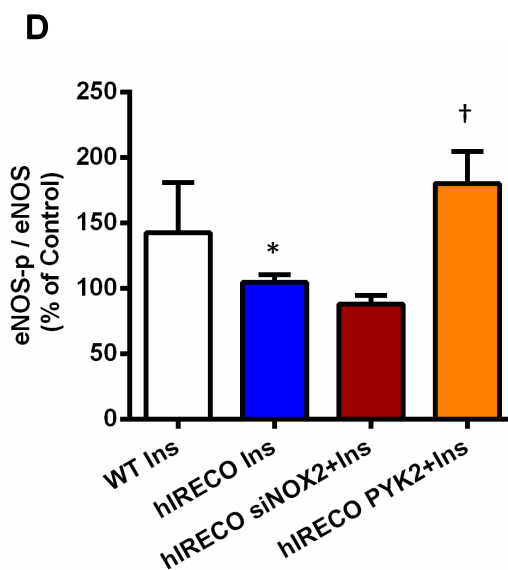
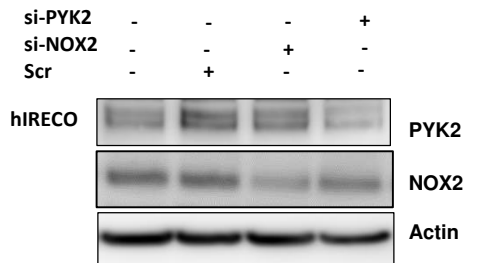
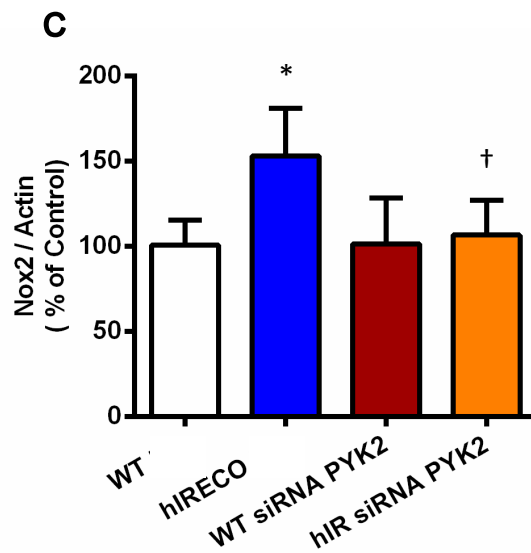
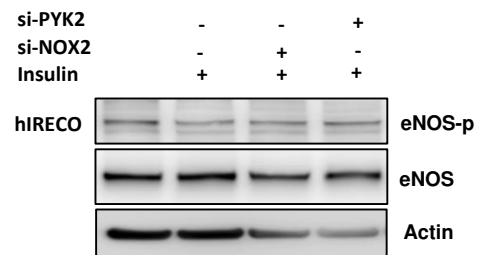
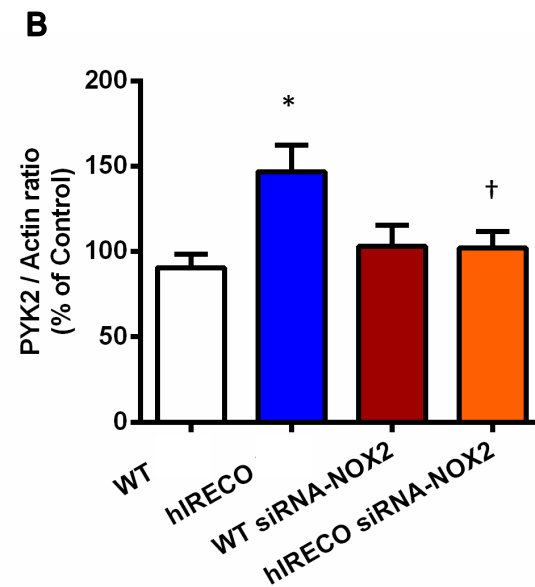
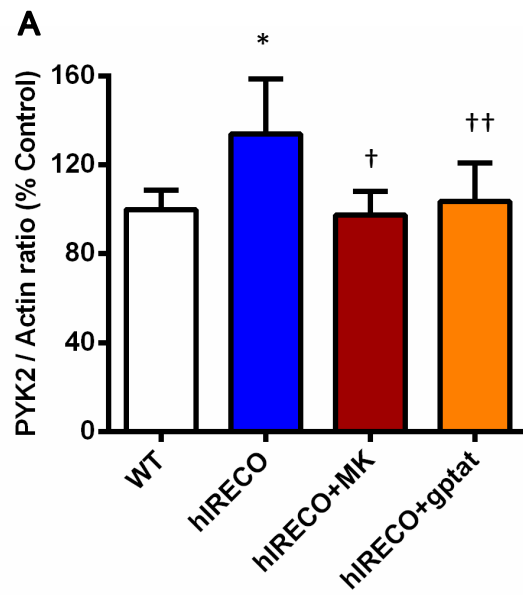
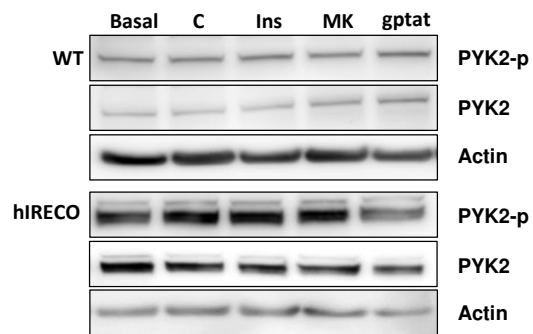
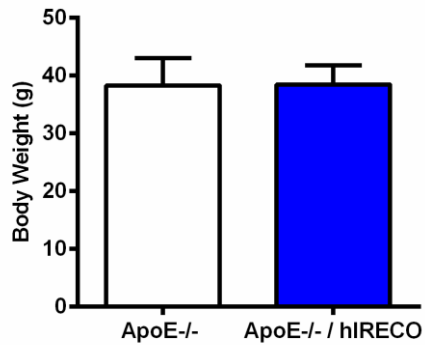
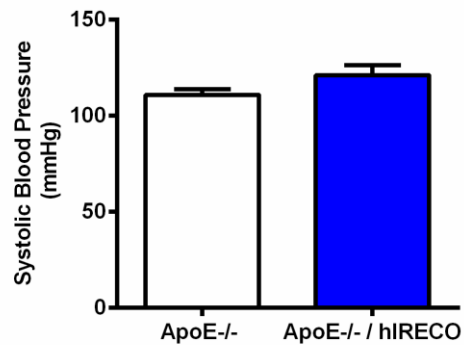
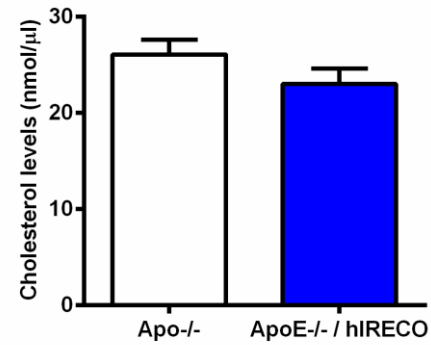
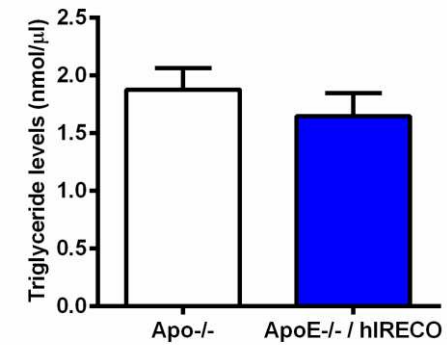
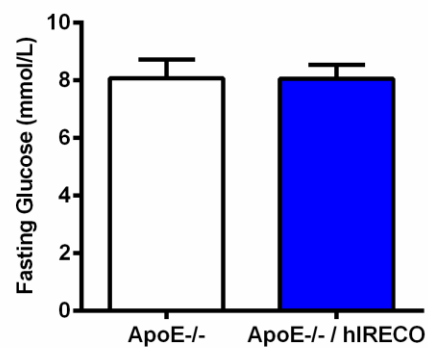
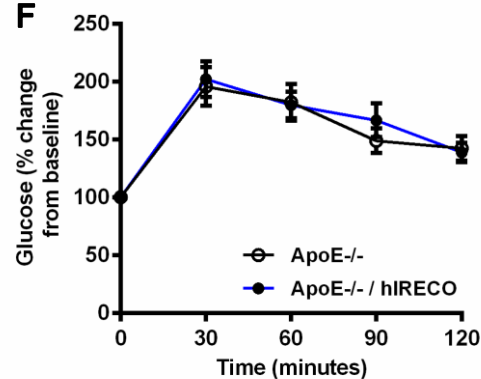
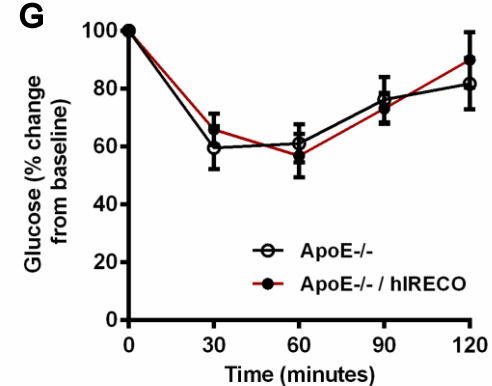
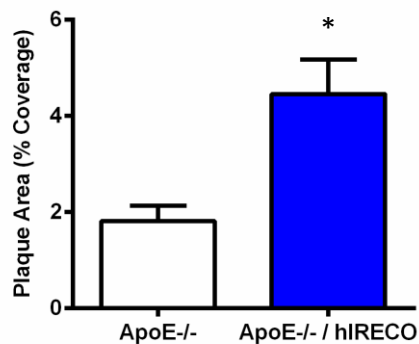
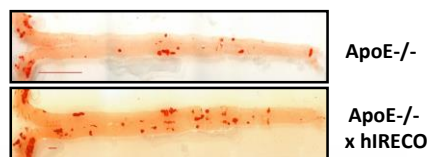
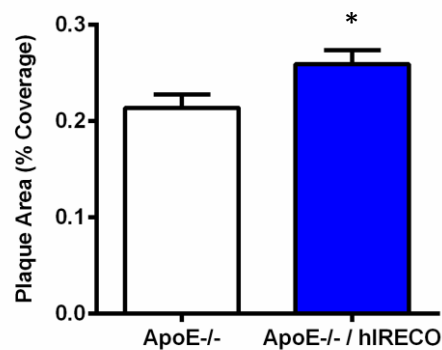
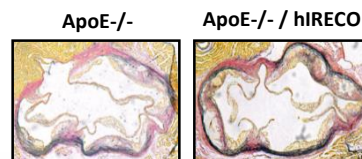


Figure 8**A****B****C****D****E****F****G****H****I****J**